
Provably Robust Streaming Models with a Sliding Window

Anonymous Authors¹

Abstract

The literature on provable robustness in machine learning has primarily focused on static prediction problems, such as image classification, in which input samples are assumed to be independent and model performance is measured as an expectation over the input distribution. Robustness certificates are derived for individual input instances with the assumption that the model is evaluated on each instance separately. However, in many deep learning applications such as online content recommendation and stock market analysis, models use historical data to make predictions. Robustness certificates based on the assumption of independent input samples are not directly applicable in such scenarios. In this work, we focus on the provable robustness of machine learning models in the context of data streams, where inputs are presented as a sequence of potentially correlated items. We derive robustness certificates for models that use a fixed-size sliding window over the input stream. Our guarantees hold for the average model performance across the entire stream and are independent of stream size, making them suitable for large data streams. We perform experiments on speech detection and human activity recognition tasks and show that our certificates can produce meaningful performance guarantees against adversarial perturbations.

1. Introduction

Deep neural network (DNN) models are increasingly being adopted for real-time decision-making and prediction tasks. Once a neural network is trained, it is often required to make fast predictions on an evolving stream of inputs, as in algorithmic trading (Zhang et al., 2017; Krauss et al., 2017; Korczak & Hemes, 2017; Fischer & Krauss, 2018;

Ozbayoglu et al., 2020), human action recognition (Yang et al., 2015; Ordonez & Roggen, 2016; Ronao & Cho, 2016) and speech detection (Graves & Schmidhuber, 2005; Dennis et al., 2019; Hsiao et al., 2020). However, despite their impressive performance, DNNs are known to malfunction under tiny perturbations of the input, designed to fool them into making incorrect predictions (Szegedy et al., 2014; Biggio et al., 2013; Goodfellow et al., 2015; Madry et al., 2018; Carlini & Wagner, 2017). This vulnerability is not limited to static models like image classifiers and has been demonstrated for streaming models as well (Braverman et al., 2021; Mladenovic et al., 2022; Ben-Eliezer et al., 2020; Ben-Eliezer & Yoge, 2020). Such input corruptions, commonly known as adversarial attacks, make DNNs especially risky for safety-critical applications of streaming models such as health monitoring (Ignatov, 2018; Stamate et al., 2017; Lee et al., 2019; Cai et al., 2020) and autonomous driving (Bojarski et al., 2016; Xu et al., 2017; Janai et al., 2020). What makes the adversarial streaming setting more challenging than the static one is that the adversary can exploit historical data to strengthen its attack. For instance, it could wait for a critical decision-making point, such as a trading algorithm making a buy/sell recommendation or an autonomous vehicle approaching a stop sign, before generating an adversarial perturbation.

Over the years, a long line of research has been dedicated to mitigating the adversarial vulnerabilities of DNNs. These methods seek to improve the empirical robustness of a model by introducing input corruptions during training (Kurakin et al., 2017; Buckman et al., 2018; Guo et al., 2018; Dhillon et al., 2018; Li & Li, 2017; Grosse et al., 2017; Gong et al., 2017). However, such empirical defenses have been shown to break down under stronger adversarial attacks (Carlini & Wagner, 2017; Athalye et al., 2018; Uesato et al., 2018; Tramer et al., 2020). This motivated the study of provable robustness in machine learning which seeks to obtain verifiable guarantees on the predictive performance of a DNN. Several certified defense techniques have been developed over the years, most notable of which are based on convex relaxation (Wong & Kolter, 2018; Raghunathan et al., 2018; Singla & Feizi, 2019; Chiang et al., 2020; Singla & Feizi, 2020), interval-bound propagation (Gowal et al., 2018; Huang et al., 2019; Dvijotham et al., 2018; Mirman et al., 2018) and randomized smoothing (Cohen et al., 2019;

¹Anonymous Institution, Anonymous City, Anonymous Region, Anonymous Country. Correspondence to: Anonymous Author <anon.email@domain.com>.

055 Lécuyer et al., 2019; Li et al., 2019; Salman et al., 2019;
 056 Levine & Feizi, 2021). Most research in provable robustness
 057 has focused on static prediction tasks like image classifica-
 058 tion and the streaming machine learning (ML) setting has
 059 not yet been considered.

060 In this work, we derive provable robustness guarantees for
 061 the streaming setting where inputs are presented as a se-
 062 quence of potentially correlated items. Our objective is
 063 to design robustness certificates that produce guarantees
 064 on the average model performance over long, potentially
 065 infinite, data streams. Our threat model is defined as a man-
 066 in-the-middle adversary present between the DNN and the
 067 data stream that can perturb the input items before they
 068 are passed to the DNN. The adversary is constrained by a
 069 limit on the average perturbation added to the inputs. We
 070 show that a DNN that randomizes the inputs before making
 071 predictions is guaranteed to achieve a certain performance
 072 level for any adversary within the threat model. Unlike
 073 many randomized smoothing-based approaches that aggre-
 074 gate predictions over several noised samples ($\sim 10^6$) of the
 075 input instance, our procedure only requires one sample of
 076 the randomized input, keeping the computational complex-
 077 ity of the DNN unchanged. Our certificates are independent
 078 of the stream length, making them suitable for large streams.
 079

080 **Technical Challenges:** Provably robustness procedures de-
 081 veloped for static tasks like image classification assume that
 082 the inputs are sampled independently from the data distri-
 083 bution. Robustness certificates are derived for individual
 084 input instances with the assumption that the DNN is applied
 085 to each instance separately and the adversarial perturbation
 086 added to one instance does not affect the DNN’s predic-
 087 tions on another. However, in the streaming ML setting, the
 088 prediction at a given time-step is dependent on past input
 089 items in the data stream and a worst-case adversary can
 090 exploit this dependence between inputs to adapt its strategy
 091 and strengthen its attack. A robustness certificate that is
 092 derived based on the assumption of independence of input
 093 samples may not hold for such correlated inputs. Thus, there
 094 is a need to design provable robustness techniques tailored
 095 specifically for the streaming ML setting.

096 Out of the existing certified robustness techniques, random-
 097 ized smoothing has become prominent due to its model-
 098 agnostic nature, scalability for high-dimensional problems
 099 (Lécuyer et al., 2019), and flexibility to adapt to different
 100 machine learning paradigms like reinforcement learning
 101 and structured outputs (Kumar et al., 2021; Wu et al., 2021;
 102 Kumar & Goldstein, 2021). This makes randomized smoothing
 103 a suitable candidate for provable robustness in stream-
 104 ing ML. However, conventional randomized smoothing ap-
 105 proaches require several evaluations ($\sim 10^6$) of the predic-
 106 tion model on different noise vectors in order to produce a
 107 robust output. This significantly increases the computational
 108 cost.

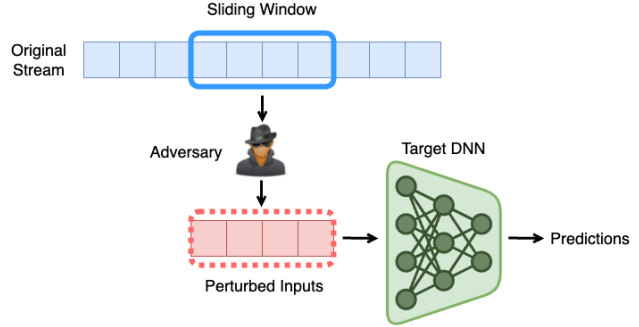


Figure 1. Adversarial Streaming Threat Model.

requirements of the model making them infeasible for real-world streaming applications which require decisions to be made in a short time frame such as high-frequency trading and autonomous driving. Our goal is to obtain robustness guarantees for a simple technique that only adds a single noise vector to the DNN’s input.

Existing works on provable robustness in reinforcement learning (Kumar et al., 2021; Wu et al., 2021) indicate that if the prediction at a given time-step is a function of the entire stream till that step, the robustness guarantees worsen with the length of the stream and become vacuous for large stream sizes. The tightness analysis of these certificates suggests that it might be difficult to achieve robustness guarantees that are independent of the stream size. However, many practical streaming models use only a bounded number of past input items in order to make predictions at a given time step. Recent work by Efroni et al. (2022) has also shown that near-optimal performance can be achieved by only observing a small number of past inputs for several real-world sequential decision-making problems. This raises the natural question:

Can we obtain better certificates if the DNN only used a fixed number of inputs from the stream?

Our Contributions: We design a robustness certificate for streaming models that use a fixed-sized sliding window over the data stream to make predictions (see Figure 1). In our setting, the DNN only uses the part of the data stream inside the window at any given time step. We certify the average performance Z of the model over a stream of size t :

$$Z = \frac{\sum_{i=1}^t f_i}{t},$$

where each f_i measures the predictive performance of the DNN at time-step i as a value in the range $[0, 1]$.

The adversary is allowed to perturb the input items inside the window at every time step separately. The strength of

110 the adversary is limited by a bound ϵ on the average size of
 111 the perturbation added:

$$\frac{\sum_{i=1}^t \sum_{k=1}^w d(x_i, x_i^k)}{wt} \leq \epsilon,$$

117 where x_i and x_i^k are the input item at time-step i and its
 118 k th adversarial perturbation respectively, w is the window
 119 size and d is a distance function to measure the size of
 120 the adversarial perturbations, e.g., $d(x_i, x_i^k) = \|x_i - x_i^k\|_2$.
 121 Our adversarial threat model is general enough to subsume
 122 the scenario where the attacker only perturbs each stream
 123 element only once as a special case where all x_i^k 's are set to
 124 some x'_i .

125 Our main theoretical result shows that the difference be-
 126 tween the clean performance of a robust streaming model
 127 \tilde{Z} and that in the presence of an adversarial attack \tilde{Z}_ϵ is
 128 bounded as follows:

$$|\tilde{Z} - \tilde{Z}_\epsilon| \leq w\psi(\epsilon), \quad (1)$$

133 where $\psi(\cdot)$ is a concave function that bounds the total varia-
 134 tion between the smoothing distributions at two input points
 135 as a function of the distance between them (condition (4)
 136 in Section 3). Such an upper bound always exists for any
 137 smoothing distribution. For example, when the distance
 138 between the points is measured using the ℓ_2 -norm and the
 139 smoothing distribution is a Gaussian $\mathcal{N}(0, \sigma^2 I)$ with
 140 variance σ^2 , then the concave upper bound is given by
 141 $\psi(\cdot) = \text{erf}(\cdot/2\sqrt{2}\sigma)$. Our robustness certificate is inde-
 142 pendent of the length of the stream and depends only on
 143 the window size w and average perturbation size ϵ . This
 144 suggests that streaming ML models with smaller window
 145 sizes are provably more robust to adversarial attacks.

146 We perform experiments on two real-world applications –
 147 human activity recognition and speech keyword detection.
 148 We use the UCI HAR dataset (Reyes-Ortiz et al., 2012) for hu-
 149 man activity recognition and the Speech commands dataset
 150 (Warden, 2018) for speech keyword detection. We train
 151 convolutional networks that take sliding windows as inputs
 152 and provide robustness guarantees for their performance. In
 153 our experiments, we consider two different scenarios for
 154 the adversary. In the first case, the adversary can perturb an
 155 input only once. In the more general second scenario, the
 156 adversary can perturb each sliding window separately, making
 157 it a powerful attacker. We develop strong adversaries
 158 for both of these scenarios and show their effectiveness in
 159 our experiments. We then show that our certificates provide
 160 meaningful robustness guarantees in the presence of such
 161 strong adversaries. Consistent with our theory, our experi-
 162 ments also demonstrate that a smaller window size w gives
 163 a stronger certificate.

2. Related Work

The adversarial streaming setup has been studied extensively in recent years. Mladenovic et al. (2022) designed an attack for transient data streams that do not allow the adversary to re-attack past input items. In their setting, the adversary only has partial knowledge of the target DNN and the perturbations applied in previous time steps are irrevocable. Their objective is to produce an adversarial attack with minimal access to the data stream and the target model. Our goal, on the other hand, is to design a provably robust method that can defend against as general and as strong an adversary as possible. We assume that the adversary has full knowledge of the parameters of the target DNN and can change the adversarial perturbations added in previous time steps. Our threat model includes transient data streams as a special case and applies even to adversaries that only have partial access to the DNN. Streaming adversarial attacks have also been studied for sampling algorithms such as Bernoulli sampling and reservoir sampling (Ben-Eliezer & Yogeav, 2020). Here, the goal of the adversary is to create a stream that is unrepresentative of the actual data distribution. Other works have studied the adversarial streaming setup for specific data analysis problems like frequency moment estimation (Ben-Eliezer et al., 2020), submodular maximization (Mitrovic et al., 2017), coresets construction and row sampling (Braverman et al., 2021). In this work, we focus on a robustness certificate for general DNN models in the streaming setting under the conventional notion of adversarial attacks in machine learning literature. We use a sliding-window computational model which has been extensively studied over several years for many streaming applications (Ganardi et al., 2019; Feigenbaum et al., 2005; Datar & Motwani, 2007). Recently Efroni et al. (2022) also showed that a short-term memory is sufficient for several real-world reinforcement learning tasks.

A closely related setting is that of adversarial reinforcement learning. Adversarial attacks have been designed that either directly corrupt the observations of the agent (Huang et al., 2017; Behzadan & Munir, 2017; Pattanaik et al., 2018) or introduce adversarial behavior in a competing agent (Gleave et al., 2020). Robust training methods, such as adding adversarial noise (Kamalaruban et al., 2020; Vinitsky et al., 2020) and training with a learned adversary in an online alternating fashion (Zhang et al., 2021), have been proposed to improve the robustness of RL agents. Several certified defenses have also been developed over the years. For instance, Zhang et al. (2020) developed a method that can certify the actions of an RL agent at each time step under a fixed adversarial perturbation budget. It can certify the total reward obtained at the end of an episode if each of the intermediate actions is certifiably robust. Our streaming formulation allows the adversary to choose the budget at each time step as long as the average perturbation size

165 remains below ϵ over time. Our framework also does not
 166 require each prediction to be robust in order to certify the
 167 average performance of the DNN. More recent works in
 168 certified RL can produce robustness guarantees on the total
 169 reward without requiring every intermediate action to be
 170 robust or the adversarial budget to be fixed (Kumar et al.,
 171 2021; Wu et al., 2021). However, these certificates degrade
 172 for longer streams and the tightness analysis of these certifi-
 173 cates indicates that this dependence on stream size may not
 174 be improved. Our goal is to keep the robustness guarantees
 175 independent of stream size so that they are suitable even for
 176 large streams.

177 The literature on provable robustness has primarily focused
 178 on static prediction problems like image classification. One
 179 of the most prominent techniques in this line of research is
 180 randomized smoothing. For a given input image, this tech-
 181 nique aggregates the output of a DNN on several noisy ver-
 182 sions of the image to produce a robust class label (Lécuyer
 183 et al., 2019; Cohen et al., 2019). This is the first approach
 184 that scaled up to high-dimensional image datasets like Im-
 185 ageNet for ℓ_2 -norm bounded adversaries.. It does not make
 186 any assumptions on the underlying neural network such as
 187 Lipschitz continuity or a specific architecture, making it
 188 suitable for conventional DNNs that are several layers deep.
 189 However, randomized smoothing also suffers some funda-
 190 mental limitations for higher norms such as the ℓ_∞ -norm
 191 (Kumar et al., 2020). Due to its flexible nature, randomized
 192 smoothing has also been adapted for tasks beyond classifi-
 193 cation, such as segmentation and deep generative modeling,
 194 with multi-dimensional and structured outputs like images,
 195 segmentation masks, and language (Kumar & Goldstein,
 196 2021). For such outputs, robustness certificates are designed
 197 in terms of a distance metric in the output space such as
 198 LPIPS distance, intersection-over-union and total variation
 199 distance. However, provable robustness in the static setting
 200 assumes a fixed budget on the size of the adversarial
 201 perturbation for each input instance and does not allow the
 202 adversary to choose a different budget for each instance. In
 203 our streaming threat model, we allow the adversary the flex-
 204 ibility of allocating the adversarial budget to different time
 205 steps in an effective way, attacking more critical input items
 206 with a higher budget and conserving its budget at other time
 207 steps. Recent work on provable robustness against Wasser-
 208 stein shifts of the data distribution allows the adversary to
 209 choose the attack budget for each instance differently (Ku-
 210 mar et al., 2022). However, unlike our streaming setting,
 211 the input instances are drawn independently from the data
 212 distribution and the adversarial perturbation applied to one
 213 instance does not impact the performance of the DNN on
 214 another.

3. Preliminaries and Notation

Streaming ML Setting: We define a data stream of size t as a sequence of input items $x_1, x_2, \dots, x_i, \dots, x_t$ generated one-by-one from an input space \mathcal{X} over discrete time steps. At each time step i , a DNN model μ makes a prediction that may depend on no more than w of the previous inputs. We refer to the contiguous block of past input items as a window $W_i \in \mathcal{X}^{\min(i,w)}$ of size w defined as follows:

$$W_i = \begin{cases} (x_1, x_2, \dots, x_i) & \text{for } i \leq w \\ (x_{i-w+1}, x_{i-w+2}, \dots, x_i) & \text{otherwise.} \end{cases}$$

The performance of the model μ at time step i is given by a function $f_i : \mathcal{X}^{\min(i,w)} \rightarrow [0, 1]$ that passes the window W_i through the model μ , compares the prediction with the ground truth and outputs a value in the range $[0, 1]$. For instance, in speech recognition, the window W_i would represent the audio from the past few seconds which gets fed to the model μ . The function $f_i = \mathbf{1}\{\mu(W_i) = y_i\}$ could indicate whether the prediction of μ matches the ground truth y_i . Similarly, in autonomous driving, we can define a performance function $f_i = \text{IoU}(\mu(W_i), y_i)$ that measures the average intersection-over-union of the segmentation mask of the surrounding environment. We define the overall performance Z of the model μ as an average over the t time-steps:

$$Z = \frac{\sum_{i=1}^t f_i}{t}.$$

Threat Model: An adversary A is present between the DNN and the data stream which can perturb the inputs with the objective of minimizing the average performance Z of the DNN (see Figure 1). Let x'_i be the perturbed input at step i . We define a constraint on the amount by which the adversary can perturb the inputs as a bound on the average distance between the original input items x_i and their perturbed versions x'_i :

$$\frac{\sum_{i=1}^t d(x_i, x'_i)}{t} \leq \epsilon, \quad (2)$$

where d is a function that measures the distance between a pair of input items from \mathcal{X} , e.g., $d(x_i, x'_i) = \|x_i - x'_i\|_2$. The adversary seeks to minimize the overall performance Z of the model without violating the above constraint, i.e.,

$$\min_{A \in \mathcal{A}_\epsilon} \sum_{i=1}^t f_i(A(x_i), A(x_{i-1}), \dots, A(x_{i-w+1}))/t,$$

where \mathcal{A}_ϵ is the set of all adversaries satisfying constraint (2). We also study another threat model where the adversary is allowed to attack an input item x_i in every window that it appears in. We denote the k -th attack of x_i as x_i^k and redefine the above constraint as follows:

$$\frac{\sum_{i=1}^t \sum_{k=1}^w d(x_i, x_i^k)}{wt} \leq \epsilon \quad (3)$$

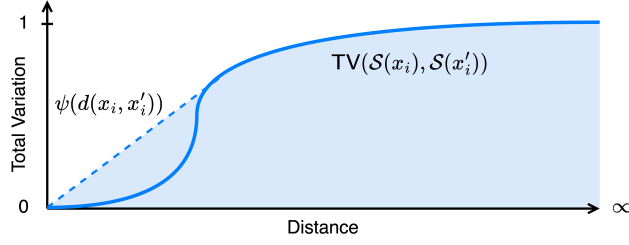


Figure 2. Constructing a concave upper bound $\psi(\cdot)$ for any smoothing distribution \mathcal{S} .

This threat model is more general than the one defined by constraint (2) because it subsumes this constraint as a special case when all x_i^k are equal to x'_i . Thus, any robustness guarantee that holds for this stronger threat model must also hold for the previous one.

Robustness Procedure: Our goal is to design a procedure that has provable robustness guarantees against the above threat models. We define a robust prediction model $\tilde{\mu}$: Given an input $x_i \in \mathcal{X}$, we sample a point \tilde{x}_i from a probability distribution $\mathcal{S}(x_i)$ around x_i (e.g., $\mathcal{N}(x_i, \sigma^2 I)$) and evaluate the model μ on \tilde{x}_i . Define the performance of $\tilde{\mu}$ at time-step i to be the expected value of f_i under the randomized inputs, i.e.,

$$\tilde{f}_i = \mathbb{E}_{\tilde{x}_i \sim \mathcal{S}(x_i)} [f_i(\tilde{x}_i, \tilde{x}_{i-1}, \dots, \tilde{x}_{i-w+1})]$$

and the overall performance as $\tilde{Z} = \sum_{i=1}^t \tilde{f}_i / t$.

Let $\psi(\cdot)$ be a concave function bounding the total variation between the distributions $\mathcal{S}(x_i)$ and $\mathcal{S}(x'_i)$ as a function of the distance between them, i.e.,

$$TV(\mathcal{S}(x_i), \mathcal{S}(x'_i)) \leq \psi(d(x_i, x'_i)). \quad (4)$$

Such a bound always exists regardless of the shape of the smoothing distribution because as the distance between the points x_i and x'_i goes from 0 to ∞ , the total variation goes from 0 to 1. A trivial concave bound could be obtained by simply taking the convex hull of the region under the total variation curve (see Figure 2). However, to find a closed-form expression for ψ , we need to analyze different smoothing distributions and distance functions separately. If the smoothing distribution is a Gaussian $\mathcal{N}(0, \sigma^2 I)$ with variance σ^2 and the distance is measured using the ℓ_2 -norm, as in all of our experiments, then $\psi(\|x_i - x'_i\|_2) = \text{erf}(\|x_i - x'_i\|_2 / 2\sqrt{2}\sigma)$, where erf is the Gauss error function. For a uniform smoothing distribution within an interval of size b in each dimension of x_i and the ℓ_1 -distance metric, $\psi(\|x_i - x'_i\|_1) = \|x_i - x'_i\|_1 / b$. See Appendix C for proof.

4. Robustness Certificate

In this section, we prove robustness guarantees for the simpler threat model defined by constraint (2) where each input item is allowed to be attacked only once. We include complete proofs of our theorems for this threat model in this section for clarity. The proofs for the more general case in the next section use similar techniques and have been included in the appendix. In the following lemma, we bound the change in the performance function \tilde{f}_i at each time-step i using the function ψ and the size of the adversarial perturbation added at each step. For the proof, we first decompose the change in the value of this function into components for each input item. Since each of these components can be expressed as the difference of the expected value of a function in the range $[0, 1]$ under two probability distributions, they can be bounded by the total variation of these distributions.

Lemma 4.1. *The change in each \tilde{f}_i under an adversary in \mathcal{A}_ϵ is bounded as*

$$|\tilde{f}_i(x_i, x_{i-1}, \dots, x_{i-s+1}) - \tilde{f}_i(x'_i, x'_{i-1}, \dots, x'_{i-s+1})| \leq \sum_{j=i}^{i-s+1} \psi(d(x_j, x'_j)),$$

where $s = \min(i, w)$.

Proof. The left-hand side of the above inequality can be re-written as:

$$\begin{aligned} & |\tilde{f}_i(x_i, x_{i-1}, \dots, x_{i-s+1}) - \tilde{f}_i(x'_i, x'_{i-1}, \dots, x'_{i-s+1})| \\ &= |\tilde{f}_i(x_i, x_{i-1}, \dots, x_{i-s+1}) - \tilde{f}_i(x'_i, x_{i-1}, \dots, x_{i-s+1}) \\ &\quad + \tilde{f}_i(x'_i, x_{i-1}, \dots, x_{i-s+1}) - \tilde{f}_i(x'_i, x'_{i-1}, \dots, x'_{i-s+1})| \\ &= \left| \sum_{j=i}^{i-s+1} \tilde{f}_i(x'_i, \dots, x_j, \dots, x_{i-s+1}) \right. \\ &\quad \left. - \tilde{f}_i(x'_i, \dots, x'_j, \dots, x_{i-s+1}) \right| \\ &\leq \sum_{j=i}^{i-s+1} |\tilde{f}_i(x'_i, \dots, x_j, \dots, x_{i-s+1}) \\ &\quad - \tilde{f}_i(x'_i, \dots, x'_j, \dots, x_{i-s+1})| \end{aligned}$$

The two terms in each summand differ only in the j th input. Thus, the j th term in the above summation can be written as the difference of the expected value of some $[0, 1]$ -function q_j under the distributions $\mathcal{S}(x_j)$ and $\mathcal{S}(x'_j)$, i.e., $|\mathbb{E}_{\tilde{x} \sim \mathcal{S}(x_j)}[q_j(\tilde{x})] - \mathbb{E}_{\tilde{x} \sim \mathcal{S}(x'_j)}[q_j(\tilde{x})]|$, which can be upper bounded by the total variation between $\mathcal{S}(x_j)$ and $\mathcal{S}(x'_j)$. Here, q_j is given by:

$$q_j(\chi) = \mathbb{E}[f_i(\tilde{x}'_i, \dots, \tilde{x}'_{j-1}, \chi, \tilde{x}_{j+1}, \dots, \tilde{x}_{i-s+1})],$$

where $\chi \in \mathcal{X}$ is the j th input item, the inputs before χ are drawn from the respective adversarially shifted smoothing distributions and the inputs after χ are drawn from the original distributions, i.e., $\tilde{x}'_i \sim \mathcal{S}(x'_i), \dots, \tilde{x}'_{j-1} \sim \mathcal{S}(x'_{j-1})$ and $\tilde{x}_{j+1} \sim \mathcal{S}(x_{j+1}), \dots, \tilde{x}_{i-s+1} \sim \mathcal{S}(x_{i-s+1})$.

Without loss of generality, assume $\mathbb{E}_{\tilde{\chi} \sim \mathcal{S}(x_j)}[q_j(\tilde{\chi})] \geq \mathbb{E}_{\tilde{\chi} \sim \mathcal{S}(x'_j)}[q_j(\tilde{\chi})]$. Then,

$$\begin{aligned}
 & |\mathbb{E}_{\tilde{\chi} \sim \mathcal{S}(x_j)}[q_j(\tilde{\chi})] - \mathbb{E}_{\tilde{\chi} \sim \mathcal{S}(x'_j)}[q_j(\tilde{\chi})]| \\
 &= \int_{\mathcal{X}} q_j(x) \mu_1(x) dx - \int_{\mathcal{X}} q_j(x) \mu_2(x) dx \\
 &\quad (\mu_1 \text{ and } \mu_2 \text{ are the PDFs of } \mathcal{S}(x_j) \text{ and } \mathcal{S}(x'_j)) \\
 &= \int_{\mathcal{X}} q_j(x) (\mu_1(x) - \mu_2(x)) dx \\
 &= \int_{\mu_1 > \mu_2} q_j(x) (\mu_1(x) - \mu_2(x)) dx \\
 &\quad - \int_{\mu_2 > \mu_1} q_j(x) (\mu_2(x) - \mu_1(x)) dx \\
 &\leq \int_{\mu_1 > \mu_2} \max_{x' \in \mathcal{X}} q_j(x') (\mu_1(x) - \mu_2(x)) dx \\
 &\quad - \int_{\mu_2 > \mu_1} \min_{x' \in \mathcal{X}} q_j(x') (\mu_2(x) - \mu_1(x)) dx \\
 &\leq \int_{\mu_1 > \mu_2} (\mu_1(x) - \mu_2(x)) dz \\
 &\quad (\text{since } \max_{x' \in \mathcal{X}} q_j(x') \leq 1 \text{ and } \min_{x' \in \mathcal{X}} q_j(x') \geq 0) \\
 &= \frac{1}{2} \int_{\mathcal{X}} |\mu_1(x) - \mu_2(x)| dx = \text{TV}(\mathcal{S}(x_1), \mathcal{S}(x_2)).
 \end{aligned}$$

The equality in the last line follows from the fact that $\int_{\mu_1 > \mu_2} (\mu_1(x) - \mu_2(x)) dx = \int_{\mu_2 > \mu_1} (\mu_2(x) - \mu_1(x)) dx = \frac{1}{2} \int_{\mathcal{X}} |\mu_1(x) - \mu_2(x)| dx$.

Therefore, from condition (4), we have:

$$\begin{aligned}
 & |\tilde{f}_i(x'_i, \dots, x_j, \dots, x_{i-w+1}) - \tilde{f}_i(x'_i, \dots, x'_j, \dots, x_{i-w+1})| \\
 &\leq \text{TV}(\mathcal{S}(x_j), \mathcal{S}(x'_j)) \leq \psi(d(x_j, x'_j)).
 \end{aligned}$$

This proves the statement of the lemma. \square

Now we use the above lemma to prove the main robustness guarantee. We first decompose the change in the average performance into the average of the differences at each time step. Then we apply lemma 4.1 to bound each difference with the function ψ of the per-step perturbation size. We then utilize the convex nature of ψ to convert this average over the performance differences to an average of perturbation sizes, which completes the proof.

Theorem 4.2. Let \tilde{Z}_ϵ to be the minimum \tilde{Z} for an adversary in \mathcal{A}_ϵ . Then,

$$|\tilde{Z} - \tilde{Z}_\epsilon| \leq w\psi(\epsilon).$$

Proof. Let \tilde{Z}' be the overall performance of \tilde{M} under an adversary. Then,

$$\begin{aligned}
 |\tilde{Z} - \tilde{Z}'| &= \left| \frac{\sum_{i=1}^t \tilde{f}_i(x_i, x_{i-1}, \dots, x_{i-s+1})}{t} \right. \\
 &\quad \left. - \frac{\sum_{i=1}^t \tilde{f}_i(x'_i, x'_{i-1}, \dots, x'_{i-s+1})}{t} \right| \\
 &\quad (\text{where } s = \min(i, w)) \\
 &\leq \frac{1}{t} \sum_{i=1}^t \left| \tilde{f}_i(x_i, x_{i-1}, \dots, x_{i-s+1}) \right. \\
 &\quad \left. - \tilde{f}_i(x'_i, x'_{i-1}, \dots, x'_{i-s+1}) \right| \\
 &\leq \sum_{i=1}^t \sum_{j=i}^{i-s+1} \psi(d(x_j, x'_j))/t \quad (\text{from lemma 4.1}) \\
 &\leq w \sum_{i=1}^t \psi(d(x_i, x'_i))/t \\
 &\quad (\text{since each term appears at most } w \text{ times}) \\
 &\leq w\psi \left(\sum_{i=1}^t d(x_i, x'_i)/t \right) \\
 &\quad (\psi \text{ is concave and Jensen's inequality})
 \end{aligned}$$

Therefore, for the worst-case adversary in \mathcal{A}_ϵ , we have

$$|\tilde{Z} - \tilde{Z}_\epsilon| \leq w\psi(\epsilon)$$

from constraint (2) on the average distance between the original and perturbed inputs. \square

Although the above certificate is designed for the sliding-window computational model for streaming applications, it may also be applied to the static tasks like classification with a fixed adversarial budget for all inputs by setting $w = 1$. In Appendix D, we compare the our bound with that obtained by Cohen et al. (2019) for an ℓ_2 -norm bounded adversary and a Gaussian smoothing distribution. While the above bound is not tight, our analysis shows that the gap with static ℓ_2 -certificate is small for meaningful robustness guarantees.

5. Attacking Each Window

Now we consider the case where the adversary is allowed to attack each window seen by the target DNN separately. The threat model in this section is defined using constraint (3). It is able to re-attack an input item x_i in each new window. Similar to the definition of a window in Section 3, define an adversarially corrupted window W'_i as:

$$W'_i = \begin{cases} (x_1^i, x_2^{i-1}, \dots, x_i^1) & \text{for } i \leq w \\ (x_{i-w+1}^w, x_{i-w+2}^{w-1}, \dots, x_i^1) & \text{otherwise,} \end{cases}$$

330 where x_i^k is the k^{th} perturbed instance of x_i .

331 Similar to the certificate derived in Section 4, we first bound
 332 the change in the per-step performance function and then
 333 use that result to prove the final robustness guarantee. We
 334 formulate the following lemma similar to Lemma 4.1 but
 335 accounting for the fact that each input item can be perturbed
 336 multiple times.
 337

Lemma 5.1. *The change in each \tilde{f}_i under an adversary in \mathcal{A}_ϵ is bounded as*

$$341 \quad |\tilde{f}_i(W_i) - \tilde{f}_i(W'_i)| \leq \sum_{j=i-s+1}^i \psi(d(x_j, x_j^{i+1-j})),$$

344 where $s = \min(i, w)$.

345 The proof is available in Appendix A.

346 We prove the same certified robustness bound as in Section 4
 347 but the ϵ here is defined according to constraint (3).

349 **Theorem 5.2.** *Let \tilde{Z}_ϵ to be the minimum \tilde{Z} for an adversary
 350 in \mathcal{A}_ϵ . Then,*

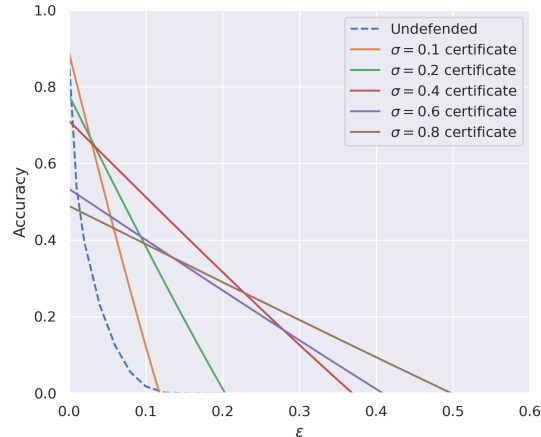
$$352 \quad |\tilde{Z} - \tilde{Z}_\epsilon| \leq w\psi(\epsilon).$$

353 The proof is available in Appendix B.

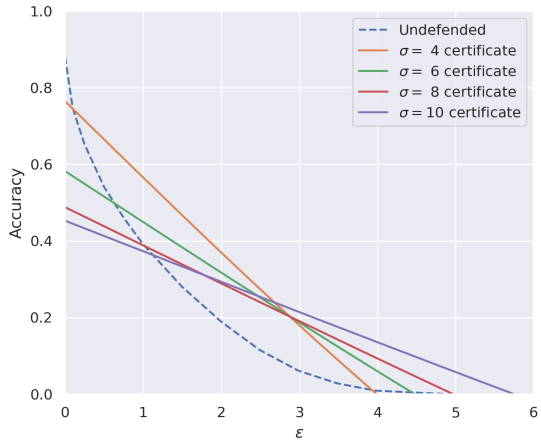
356 6. Experiments

357 We test our certificates for two streaming tasks – speech
 358 keyword detection and human activity recognition. We use
 359 a subset of the Speech commands dataset (Warden, 2018)
 360 for our speech keyword detection task. The subset we use
 361 contains ten keyword classes, corresponding to utterances
 362 of numbers from zero to nine recorded at a sample rate of
 363 16 kHz. This dataset also contains noise clips such as audio
 364 of running tap water and exercise bike. We add these noise
 365 clips to the speech audio to simulate real-world scenarios
 366 and stitch them together to generate longer audio clips. We
 367 use the UCI HAR dataset (Reyes-Ortiz et al., 2012) for
 368 human activity recognition. This contains a 6-D triaxial
 369 accelerometer and gyroscope readings measured with
 370 human subjects. The objective in HAR is to recognize various
 371 human activities based on sensor readings. The UCI HAR
 372 dataset contains signals recorded at 50 Hz that correspond
 373 to six human activities such as standing, sitting, laying,
 374 walking, walking up, and walking down.

376 We use the M5 network described in (Dai et al., 2017) with
 377 an SGD optimizer and an initial learning rate of 0.1, which
 378 we anneal using a cosine scheduler. For the speech detection
 379 task, we train a M5 network with 128 channels for 30 epochs
 380 with a batch size of 128. For the human activity recognition
 381 task, we use a M5 network with 32 channels for 30 epochs
 382 with a batch size of 256. We apply isotropic Gaussian noise
 383 for smoothing and use the ℓ_2 -norm to define the average
 384



(a) Speech keyword detection



(b) Human activity recognition

Figure 3. Certificates against online adversarial attacks for varying smoothing noises. Here we can perturb each input only once. The average size of perturbation is computed as per equation 2.

distance measure d . For the speech keyword detection task, we use smoothing noises with standard deviations of 0.1, 0.2, 0.4, 0.6, and 0.8. For the human activity recognition task, we use smoothing noises with standard deviations of 4, 6, 8, and 10. See Appendix E for more details on the experiments. We compute certificates for both scenarios, where the input is attacked only once and where each window can be attacked with the ability to re-attack inputs. These experiments show that our certificates provide meaningful guarantees against adversarial perturbations.

6.1. Attacking an input only once

We evaluate the robustness of undefended models using a custom-made attack that is constrained by the ℓ_2 -norm budget, as described in equation 2. To adhere to this constraint at each time-step j , the attacker must only perturb

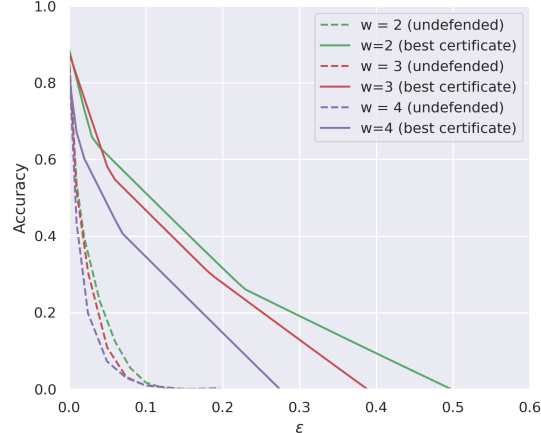
385 **Algorithm 1** Our streaming attack
 386 **Input:** time-step j , clean inputs $x_j, x_{j-1}, \dots, x_{j-w+1}$,
 387 perturbed inputs $x'_{j-1}, \dots, x'_{j-w+1}$, attack budget ϵ ,
 388 search parameter $\alpha \in \mathbb{N}$.
 389 $d_{j-1} = \sum_{i=1}^{j-1} d(x_i, x'_i)$
 390 $\text{budget}_j = j\epsilon - d_{j-1}$
 391 **for** $i = 0$ **to** α **do**
 392 $\epsilon' = \frac{i}{\alpha} \cdot \text{budget}_j$
 393 $x = \arg \min_x f_j(x, \dots, x'_{j-w+1})$ s.t. $d(x, x_j) \leq \epsilon'$
 394 **if** $f_j(x'_j, \dots, x'_{j-w+1}) = 0$ **then**
 395 $x'_j = x$
 396 **break**
 397 **else**
 398 $x'_j = x_j$
 399 **end if**
 400 **end for**

403 the input x_j , since the previous inputs $(x_{j-w+1}, \dots, x_{j-1})$
 404 have already been perturbed. This creates a significant challenge
 405 in creating a strong adversary. We design an adversary that only perturbs
 406 the last input x_j at every time-step j using projected gradient descent to minimize f_j . In our
 407 experiments, we set $f_j = 1$ if the model outputs the correct class and $f_j = 0$ when the model misclassifies. We
 408 linearly search using grid search parameter α for the smallest distance $d(x_j, x'_j)$ such that the input $(x'_{j-w+1}, \dots, x'_j)$
 409 leads to a misclassification at time-step j . We perturb x_j if
 410 $(x'_{j-w+1}, \dots, x'_j)$ leads to misclassification and the average
 411 distance budget at time-step j is less than ϵ . Else, we do not
 412 perturb x_j . In this manner, our attack perturbs the streaming
 413 input in a greedy fashion. See Algorithm 1 for details.

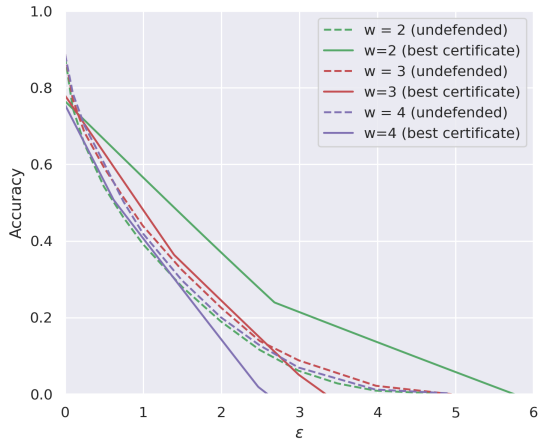
417 We conduct our streaming attack on the keyword recognition
 418 task with a window size of $w = 2$, where each input x_j
 419 is a 4000-dimensional vector in the range $[0, 1]$. We also
 420 perform the attack on the human activity recognition task
 421 with $w = 2$, where each input x_j is a 250x6-dimensional
 422 matrix. We use search parameter $\alpha = 15$. We plot the
 423 results of our certificates for various smoothing noises (see
 424 Figure 3). Note that the attack budget ϵ is calculated as
 425 per the definition in equation 2. In Figure 4, we also plot
 426 our best certificates across various smoothing noises for
 427 different window sizes w . This plot supports our theory
 428 that streaming models with smaller window sizes are more
 429 robust to adversarial perturbations. Figure 7 in Appendix
 430 F shows that the empirical performance of smooth models
 431 after the online adversarial attack is lower bound by our
 432 certificates. These plots validate our certificates.
 433

434 6.2. Attacking each window

435 Now, we perform experiments for the attack setting de-
 436 scribed in Section 5. Note that here we need to calculate the
 437 attack budget ϵ based on equation 3. In this setting, we can
 438



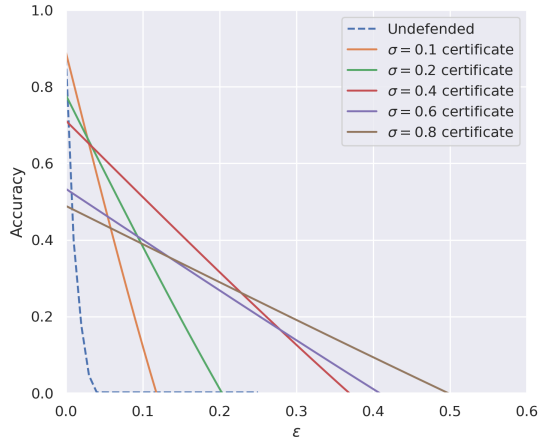
(a) Speech keyword detection



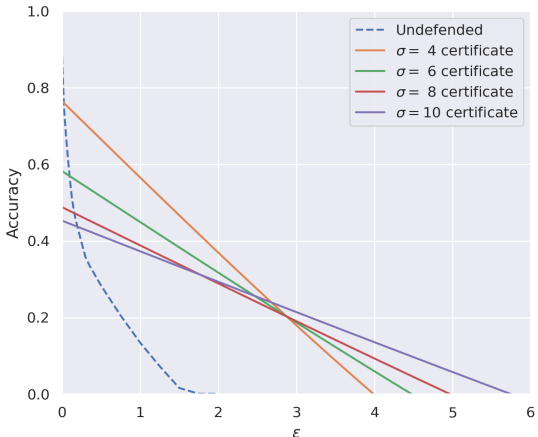
(b) Human activity recognition

Figure 4. Best certificates across varying smoothing noises for different window sizes. Streaming models with smaller window sizes are more robust to adversarial perturbations.

re-attack an input for every window, making it a stronger attack. To attack the undefended models, we search for window perturbations that lead to misclassification using a minimum distance budget. Similar to our previous attack in Section 6.1, we only perturb a window at time-step j if the average window distance at time-step j is less than ϵ . Also, we do not perturb a window if the window can not be perturbed to reduce the performance f_j . In Figure 5, we plot our certificates for this attack setting along with the accuracy of the undefended model for different attack budgets. These experiments show that our certificates produce meaningful performance guarantees against adversarial perturbations even if an attacker has the ability to re-attack the inputs.



(a) Speech keyword detection



(b) Human activity recognition

Figure 5. Certificates against online adversarial attacks for varying smoothing noises. Here we attack each window with the ability to re-attack inputs. The average size of perturbation is computed as per equation 3.

7. Conclusion

In this work, we design provable robustness guarantees for streaming machine learning models with a sliding window. Our certificates provide a lower bound on the average performance of a streaming DNN model in the presence of an adversary. The adversarial budget in our threat model is defined in terms of the average size of the perturbations added to the input items across the entire stream. This allows the adversary to allocate a different budget to each input item and leads to a more general threat model than the static setting. Our certificates are independent of the stream length and can handle long, potentially infinite, streams. They are also applicable for adversaries that are allowed to re-attack past inputs leading to strong robustness guarantees covering a wide range of attack strategies.

Our robustness procedure simply augments the inputs with random noise. Unlike conventional randomized smoothing techniques, our method only requires one noised sample per prediction keeping the computational requirements of the DNN model unchanged. It does not make any assumptions about the DNN model such as Lipschitz continuity or a specific architecture and is applicable for conventional DNNs that are several layers deep. Our experimental results show that our certificates can obtain meaningful robustness guarantees for real-world streaming applications. Our results show that the certified performance of a robust model depends only on the window size and smaller windows lead to models that are provably more robust than larger windows.

To the best of our knowledge, this is the first attempt at designing adversarial robustness certificates for the streaming setting. We note that our robustness guarantees are not proven to be tight and could be improved upon by future work. We hope our work inspires further investigation into provable robustness methods for streaming ML models.

References

Athalye, A., Carlini, N., and Wagner, D. Obfuscated gradients give a false sense of security: Circumventing defenses to adversarial examples. In Dy, J. and Krause, A. (eds.), *Proceedings of the 35th International Conference on Machine Learning*, volume 80 of *Proceedings of Machine Learning Research*, pp. 274–283, Stockholmsmässan, Stockholm Sweden, 10–15 Jul 2018. PMLR.

Behzadan, V. and Munir, A. Vulnerability of deep reinforcement learning to policy induction attacks. In Perner, P. (ed.), *Machine Learning and Data Mining in Pattern Recognition - 13th International Conference, MLD-M 2017, New York, NY, USA, July 15-20, 2017, Proceedings*, volume 10358 of *Lecture Notes in Computer Science*, pp. 262–275. Springer, 2017. doi: 10.1007/978-3-319-62416-7_19. URL https://doi.org/10.1007/978-3-319-62416-7_19.

Ben-Eliezer, O. and Yoge, E. The adversarial robustness of sampling. In Suciu, D., Tao, Y., and Wei, Z. (eds.), *Proceedings of the 39th ACM SIGMOD-SIGACT-SIGAI Symposium on Principles of Database Systems, PODS 2020, Portland, OR, USA, June 14-19, 2020*, pp. 49–62. ACM, 2020. doi: 10.1145/3375395.3387643. URL <https://doi.org/10.1145/3375395.3387643>.

Ben-Eliezer, O., Jayaram, R., Woodruff, D. P., and Yoge, E. A framework for adversarially robust streaming algorithms. In Suciu, D., Tao, Y., and Wei, Z. (eds.), *Proceedings of the 39th ACM SIGMOD-SIGACT-SIGAI Symposium on Principles of Database Systems, PODS 2020, Portland, OR, USA, June 14-19, 2020*, pp. 63–80. ACM,

- 495 2020. doi: 10.1145/3375395.3387658. URL <https://doi.org/10.1145/3375395.3387658>.
- 496
- 497
- 498 Biggio, B., Corona, I., Maiorca, D., Nelson, B., Srndic,
499 N., Laskov, P., Giacinto, G., and Roli, F. Evasion at-
500 tacks against machine learning at test time. In Blockeel,
501 H., Kersting, K., Nijssen, S., and Zelezný, F. (eds.), *Ma-
502 chine Learning and Knowledge Discovery in Databases
503 - European Conference, ECML PKDD 2013, Prague,
504 Czech Republic, September 23-27, 2013, Proceedings,
505 Part III*, volume 8190 of *Lecture Notes in Computer
506 Science*, pp. 387–402. Springer, 2013. doi: 10.1007/
507 978-3-642-40994-3_25. URL https://doi.org/10.1007/978-3-642-40994-3_25.
- 508
- 509 Bojarski, M., Testa, D. D., Dworakowski, D., Firner,
510 B., Flepp, B., Goyal, P., Jackel, L. D., Monfort, M.,
511 Muller, U., Zhang, J., Zhang, X., Zhao, J., and Zieba,
512 K. End to end learning for self-driving cars. *CoRR*,
513 abs/1604.07316, 2016. URL <http://arxiv.org/abs/1604.07316>.
- 514
- 515 Braverman, V., Hassidim, A., Matias, Y., Schain, M., Silwal,
516 S., and Zhou, S. Adversarial robustness of streaming al-
517 gorithms through importance sampling. In Beygelzimer,
518 A., Dauphin, Y., Liang, P., and Vaughan, J. W. (eds.),
519 *Advances in Neural Information Processing Systems*,
520 2021. URL https://openreview.net/forum?id=83A-0x6Pfi_.
- 521
- 522 Buckman, J., Roy, A., Raffel, C., and Goodfellow, I. J.
523 Thermometer encoding: One hot way to resist adversarial
524 examples. In *6th International Conference on Learning
525 Representations, ICLR 2018, Vancouver, BC, Canada,
526 April 30 - May 3, 2018, Conference Track Proceedings*,
527 2018.
- 528
- 529 Cai, L., Gao, J., and Zhao, D. A review of the applica-
530 tion of deep learning in medical image classification and
531 segmentation. *Annals of translational medicine*, 8(11),
532 2020.
- 533
- 534 Carlini, N. and Wagner, D. A. Adversarial examples are
535 not easily detected: Bypassing ten detection methods.
536 In *Proceedings of the 10th ACM Workshop on Artificial
537 Intelligence and Security, AISec@CCS 2017, Dallas, TX,
538 USA, November 3, 2017*, pp. 3–14, 2017.
- 539
- 540 Chiang, P.-y., Ni, R., Abdelkader, A., Zhu, C., Studer,
541 C., and Goldstein, T. Certified defenses for adver-
542 sarial patches. In *8th International Conference on Learning
543 Representations*, 2020.
- 544
- 545 Cohen, J., Rosenfeld, E., and Kolter, Z. Certified adversarial
546 robustness via randomized smoothing. In Chaudhuri, K.
547 and Salakhutdinov, R. (eds.), *Proceedings of the 36th In-
548 ternational Conference on Machine Learning*, volume 97
549 of *Proceedings of Machine Learning Research*, pp. 1310–
1320, Long Beach, California, USA, 09–15 Jun 2019.
PMLR.
- 550
- Dai, W., Dai, C., Qu, S., Li, J., and Das, S. Very deep con-
551 volutional neural networks for raw waveforms. In *2017
552 IEEE international conference on acoustics, speech and
553 signal processing (ICASSP)*, pp. 421–425. IEEE, 2017.
- Datar, M. and Motwani, R. *The Sliding-Window Compu-
554 tation Model and Results*, pp. 149–167. Springer US,
555 Boston, MA, 2007. ISBN 978-0-387-47534-9. doi:
556 10.1007/978-0-387-47534-9_8. URL https://doi.org/10.1007/978-0-387-47534-9_8.
- Dennis, D., Acar, D. A. E., Mandikal, V., Sadasivan,
557 V. S., Saligrama, V., Simhadri, H. V., and Jain, P.
558 Shallow rnn: Accurate time-series classification
559 on resource constrained devices. In Wallach, H.,
560 Larochelle, H., Beygelzimer, A., d’Alché-Buc, F.,
561 Fox, E., and Garnett, R. (eds.), *Advances in Neural
562 Information Processing Systems*, volume 32. Curran As-
563 sociates, Inc., 2019. URL <https://proceedings.neurips.cc/paper/2019/file/76d7c0780ceb8fbf964c102ebc16d75f-Paper.pdf>.
- Dhillon, G. S., Azizzadenesheli, K., Lipton, Z. C., Bernstein,
564 J., Kossaifi, J., Khanna, A., and Anandkumar, A. Stochas-
565 tic activation pruning for robust adversarial defense. In
566 *6th International Conference on Learning Representa-
567 tions, ICLR 2018, Vancouver, BC, Canada, April 30 -
568 May 3, 2018, Conference Track Proceedings*, 2018.
- Dvijotham, K., Gowal, S., Stanforth, R., Arandjelovic, R.,
569 O’Donoghue, B., Uesato, J., and Kohli, P. Training veri-
570 fied learners with learned verifiers, 2018.
- Efroni, Y., Jin, C., Krishnamurthy, A., and Miryoosefi, S.
571 Provably reinforcement learning with a short-term mem-
572 ory. In Chaudhuri, K., Jegelka, S., Song, L., Szepesvári,
573 C., Niu, G., and Sabato, S. (eds.), *International Confer-
574 ence on Machine Learning, ICML 2022, 17-23 July 2022,
575 Baltimore, Maryland, USA*, volume 162 of *Proceedings
576 of Machine Learning Research*, pp. 5832–5850. PMLR,
577 2022. URL <https://proceedings.mlr.press/v162/efroni22a.html>.
- Feigenbaum, J., Kannan, S., and Zhang, J. Computing diameter in the streaming and sliding-window mod-
578 els. *Algorithmica*, 41(1):25–41, 2005. doi: 10.1007/s00453-004-1105-2. URL <https://doi.org/10.1007/s00453-004-1105-2>.
- Fischer, T. and Krauss, C. Deep learning with
579 long short-term memory networks for financial mar-
580 ket predictions. *European Journal of Operational
581 Research*, 2020.

- 550 Research, 270(2):654–669, 2018. ISSN 0377-
 551 2217. doi: <https://doi.org/10.1016/j.ejor.2017.11.054>. URL <https://www.sciencedirect.com/science/article/pii/S0377221717310652>.
- 552 Ganardi, M., Hucke, D., and Lohrey, M. Derandomization for sliding window algorithms with strict correctness. In van Bevern, R. and Kucherov, G. (eds.), *Computer Science - Theory and Applications - 14th International Computer Science Symposium in Russia, CSR 2019, Novosibirsk, Russia, July 1-5, 2019, Proceedings*, volume 11532 of *Lecture Notes in Computer Science*, pp. 237–249. Springer, 2019. doi: 10.1007/978-3-030-19955-5_21. URL https://doi.org/10.1007/978-3-030-19955-5_21.
- 553 Gleave, A., Dennis, M., Wild, C., Kant, N., Levine, S., and Russell, S. Adversarial policies: Attacking deep reinforcement learning. In *8th International Conference on Learning Representations, ICLR 2020, Addis Ababa, Ethiopia, April 26-30, 2020*. OpenReview.net, 2020. URL <https://openreview.net/forum?id=HJgEMpVFwB>.
- 554 Gong, Z., Wang, W., and Ku, W. Adversarial and clean data are not twins. *CoRR*, abs/1704.04960, 2017.
- 555 Goodfellow, I. J., Shlens, J., and Szegedy, C. Explaining and harnessing adversarial examples. In *3rd International Conference on Learning Representations, ICLR 2015, San Diego, CA, USA, May 7-9, 2015, Conference Track Proceedings*, 2015.
- 556 Gowal, S., Dvijotham, K., Stanforth, R., Bunel, R., Qin, C., Uesato, J., Arandjelovic, R., Mann, T., and Kohli, P. On the effectiveness of interval bound propagation for training verifiably robust models, 2018.
- 557 Graves, A. and Schmidhuber, J. Framewise phoneme classification with bidirectional lstm and other neural network architectures. *Neural Networks*, 18(5):602–610, 2005. ISSN 0893-6080. doi: <https://doi.org/10.1016/j.neunet.2005.06.042>. URL <https://www.sciencedirect.com/science/article/pii/S0893608005001206>. IJCNN 2005.
- 558 Grosse, K., Manoharan, P., Papernot, N., Backes, M., and McDaniel, P. D. On the (statistical) detection of adversarial examples. *CoRR*, abs/1702.06280, 2017.
- 559 Guo, C., Rana, M., Cissé, M., and van der Maaten, L. Countering adversarial images using input transformations. In *6th International Conference on Learning Representations, ICLR 2018, Vancouver, BC, Canada, April 30 - May 3, 2018, Conference Track Proceedings*, 2018.
- 560 Hsiao, R., Can, D., Ng, T., Travadi, R., and Ghoshal, A. Online automatic speech recognition with listen, attend and spell model. *IEEE Signal Processing Letters*, 27: 1889–1893, 2020.
- 561 Huang, P., Stanforth, R., Welbl, J., Dyer, C., Yogatama, D., Gowal, S., Dvijotham, K., and Kohli, P. Achieving verified robustness to symbol substitutions via interval bound propagation. In *Proceedings of the 2019 Conference on Empirical Methods in Natural Language Processing and the 9th International Joint Conference on Natural Language Processing, EMNLP-IJCNLP 2019, Hong Kong, China, November 3-7, 2019*, pp. 4081–4091, 2019. doi: 10.18653/v1/D19-1419. URL <https://doi.org/10.18653/v1/D19-1419>.
- 562 Huang, S. H., Papernot, N., Goodfellow, I. J., Duan, Y., and Abbeel, P. Adversarial attacks on neural network policies. In *5th International Conference on Learning Representations, ICLR 2017, Toulon, France, April 24-26, 2017, Workshop Track Proceedings*. OpenReview.net, 2017. URL <https://openreview.net/forum?id=ryvlRyBK1>.
- 563 Ignatov, A. Real-time human activity recognition from accelerometer data using convolutional neural networks. *Applied Soft Computing*, 62:915–922, 2018. ISSN 1568-4946. doi: <https://doi.org/10.1016/j.asoc.2017.09.027>. URL <https://www.sciencedirect.com/science/article/pii/S1568494617305665>.
- 564 Janai, J., Güney, F., Behl, A., Geiger, A., et al. Computer vision for autonomous vehicles: Problems, datasets and state of the art. *Foundations and Trends® in Computer Graphics and Vision*, 12(1-3):1–308, 2020.
- 565 Kamalaruban, P., Huang, Y.-T., Hsieh, Y.-P., Rolland, P., Shi, C., and Cevher, V. Robust reinforcement learning via adversarial training with langevin dynamics. In Larochelle, H., Ranzato, M., Hadsell, R., Balcan, M. F., and Lin, H. (eds.), *Advances in Neural Information Processing Systems*, volume 33, pp. 8127–8138. Curran Associates, Inc., 2020.
- 566 Korczak, J. and Hemes, M. Deep learning for financial time series forecasting in a-trader system. In *2017 Federated Conference on Computer Science and Information Systems (FedCSIS)*, pp. 905–912, 2017. doi: 10.15439/2017F449.
- 567 Krauss, C., Do, X. A., and Huck, N. Deep neural networks, gradient-boosted trees, random forests: Statistical arbitrage on the s&p 500. *European Journal of Operational Research*, 259(2):689–702, 2017. ISSN 0377-2217. doi: <https://doi.org/10.1016/j.ejor.2016.10.031>. URL <https://www.sciencedirect.com/science/article/pii/S0377221716308657>.

- 605 Kumar, A. and Goldstein, T. Center smoothing: Certified ro-
 606 bustness for networks with structured outputs. *Advances*
 607 in *Neural Information Processing Systems*, 34, 2021.
- 608
- 609 Kumar, A., Levine, A., Goldstein, T., and Feizi, S. Curse of
 610 dimensionality on randomized smoothing for certifiable
 611 robustness. In *Proceedings of the 37th International*
 612 *Conference on Machine Learning, ICML 2020, 13-18*
 613 *July 2020, Virtual Event*, volume 119 of *Proceedings*
 614 of *Machine Learning Research*, pp. 5458–5467. PMLR,
 615 2020. URL <http://proceedings.mlr.press/v119/kumar20b.html>.
- 616
- 617 Kumar, A., Levine, A., and Feizi, S. Policy smoothing
 618 for provably robust reinforcement learning. *CoRR*,
 619 abs/2106.11420, 2021. URL <https://arxiv.org/abs/2106.11420>.
- 620
- 621 Kumar, A., Levine, A., Goldstein, T., and Feizi, S. Certi-
 622 fying model accuracy under distribution shifts. *CoRR*,
 623 abs/2201.12440, 2022. URL <https://arxiv.org/abs/2201.12440>.
- 624
- 625 Kurakin, A., Goodfellow, I. J., and Bengio, S. Adver-
 626 sarial machine learning at scale. In *5th International*
 627 *Conference on Learning Representations, ICLR 2017,*
 628 *Toulon, France, April 24-26, 2017, Conference Track*
 629 *Proceedings*, 2017. URL <https://openreview.net/forum?id=BJm4T4Kgx>.
- 630
- 631 Lécyuer, M., Atlidakis, V., Geambasu, R., Hsu, D., and
 632 Jana, S. Certified robustness to adversarial examples
 633 with differential privacy. In *2019 IEEE Symposium on*
 634 *Security and Privacy, SP 2019, San Francisco, CA, USA,*
 635 *May 19-23, 2019*, pp. 656–672, 2019.
- 636
- 637 Lee, G., Nho, K., Kang, B., Sohn, K.-A., and Kim, D.
 638 Predicting alzheimer’s disease progression using multi-
 639 modal deep learning approach. *Scientific reports*, 9(1):
 640 1–12, 2019.
- 641
- 642 Levine, A. and Feizi, S. Improved, deterministic smoothing
 643 for L1 certified robustness. *CoRR*, abs/2103.10834, 2021.
 644 URL <https://arxiv.org/abs/2103.10834>.
- 645
- 646 Li, B., Chen, C., Wang, W., and Carin, L. Certified ad-
 647 versarial robustness with additive noise. In *Advances*
 648 in *Neural Information Processing Systems 32: Annual*
 649 *Conference on Neural Information Processing Systems*
 650 *2019, NeurIPS 2019, 8-14 December 2019, Vancouver,*
 651 *BC, Canada*, pp. 9459–9469, 2019.
- 652
- 653 Li, D., Langlois, T. R., and Zheng, C. Scene-aware audio
 654 for 360 videos. *ACM Transactions on Graphics (TOG)*,
 655 37(4):1–12, 2018.
- 656
- 657 Li, X. and Li, F. Adversarial examples detection in deep
 658 networks with convolutional filter statistics. In *IEEE In-*
 659 *ternational Conference on Computer Vision, ICCV 2017,*
 660 *Venice, Italy, October 22-29, 2017*, pp. 5775–5783, 2017.
- 661
- 662 Madry, A., Makelov, A., Schmidt, L., Tsipras, D., and
 663 Vladu, A. Towards deep learning models resistant to
 664 adversarial attacks. In *6th International Conference on*
 665 *Learning Representations, ICLR 2018, Vancouver, BC,*
 666 *Canada, April 30 - May 3, 2018, Conference Track*
 667 *Proceedings*, 2018.
- 668
- 669 Mirman, M., Gehr, T., and Vechev, M. Differentiable
 670 abstract interpretation for provably robust neural
 671 networks. In Dy, J. and Krause, A. (eds.), *Pro-*
 672 *ceedings of the 35th International Conference on Ma-*
 673 *chine Learning*, volume 80 of *Proceedings of Machine*
 674 *Learning Research*, pp. 3578–3586. PMLR, 10–15 Jul
 675 2018. URL <http://proceedings.mlr.press/v80/mirman18b.html>.
- 676
- 677 Mitrovic, S., Bogunovic, I., Norouzi-Fard, A., Tarnawski, J.,
 678 and Cevher, V. Streaming robust submodular maximiza-
 679 tion: A partitioned thresholding approach. In Guyon, I.,
 680 von Luxburg, U., Bengio, S., Wallach, H. M., Fergus, R.,
 681 Vishwanathan, S. V. N., and Garnett, R. (eds.), *Ad-*
 682 *vances in Neural Information Processing Systems 30: Annu-*
 683 *al Conference on Neural Information Processing Systems*
 684 *2017, December 4-9, 2017, Long Beach, CA, USA*, pp.
 685 4557–4566, 2017. URL <https://proceedings.neurips.cc/paper/2017/hash/3baa271bc35fe054c86928f7016e8ae6-Abstract.html>.
- 686
- 687 Mladenovic, A., Bose, J., berard, H., Hamilton, W. L.,
 688 Lacoste-Julien, S., Vincent, P., and Gidel, G. On-
 689 line adversarial attacks. In *International Conference*
 690 *on Learning Representations*, 2022. URL https://openreview.net/forum?id=bYGSzbCM_i.
- 691
- 692 Ordóñez, F. J. and Roggen, D. Deep convolutional and
 693 lstm recurrent neural networks for multimodal wearable
 694 activity recognition. *Sensors*, 16(1), 2016. ISSN 1424-
 695 8220. doi: 10.3390/s16010115. URL <https://www.mdpi.com/1424-8220/16/1/115>.
- 696
- 697 Ozbayoglu, A. M., Gudelek, M. U., and Sezer, O. B. Deep
 698 learning for financial applications: A survey. *Applied Soft*
 699 *Computing*, 93:106384, 2020.
- 700
- 701 Pattanaik, A., Tang, Z., Liu, S., Bommannan, G., and
 702 Chowdhary, G. Robust deep reinforcement learning
 703 with adversarial attacks. In André, E., Koenig, S., Das-
 704 tani, M., and Sukthankar, G. (eds.), *Proceedings of the*
 705 *17th International Conference on Autonomous Agents*
 706 *and MultiAgent Systems, AAMAS 2018, Stockholm, Swe-*
 707 *den, July 10-15, 2018*, pp. 2040–2042. International

- 660 Foundation for Autonomous Agents and Multiagent Systems Richland, SC, USA / ACM, 2018. URL <http://dl.acm.org/citation.cfm?id=3238064>.
 661
 662
 663
- 664 Raghunathan, A., Steinhardt, J., and Liang, P. Semidefinite relaxations for certifying robustness to adversarial examples. In *Proceedings of the 32nd International Conference on Neural Information Processing Systems*, NIPS'18, pp. 10900–10910, Red Hook, NY, USA, 2018. Curran Associates Inc.
 665
 666
 667
 668
 669
- 670 Reyes-Ortiz, J., Anguita, D., Ghio, A., Oneto, L., and Parra, X. Uci machine learning repository: Human activity recognition using smartphones data set, 2012.
 671
 672
 673
- 674 Ronao, C. A. and Cho, S.-B. Human activity recognition with smartphone sensors using deep learning neural networks. *Expert Systems with Applications*, 59:235–244, 2016. ISSN 0957-4174. doi: <https://doi.org/10.1016/j.eswa.2016.04.032>. URL <https://www.sciencedirect.com/science/article/pii/S0957417416302056>.
 675
 676
 677
 678
 679
- 680 Salman, H., Li, J., Razenshteyn, I. P., Zhang, P., Zhang, H., Bubeck, S., and Yang, G. Provably robust deep learning via adversarially trained smoothed classifiers. In *Advances in Neural Information Processing Systems 32: Annual Conference on Neural Information Processing Systems 2019, NeurIPS 2019, 8-14 December 2019, Vancouver, BC, Canada*, pp. 11289–11300, 2019.
 681
 682
 683
 684
 685
 686
 687
 688
 689
- 690 Singla, S. and Feizi, S. Robustness certificates against adversarial examples for relu networks. *CoRR*, abs/1902.01235, 2019.
 691
 692
 693
 694
 695
 696
 697
 698
 699
- 700 Singla, S. and Feizi, S. Second-order provable defenses against adversarial attacks. In *Proceedings of the 37th International Conference on Machine Learning, ICML 2020, 13-18 July 2020, Virtual Event*, volume 119 of *Proceedings of Machine Learning Research*, pp. 8981–8991. PMLR, 2020. URL <http://proceedings.mlr.press/v119/singla20a.html>.
 701
 702
 703
 704
 705
 706
 707
- 708 Stamate, C., Magoulas, G., Kueppers, S., Nomikou, E., Daskalopoulos, I., Luchini, M., Moussouri, T., and Rousos, G. Deep learning parkinson's from smartphone data. In *2017 IEEE International Conference on Pervasive Computing and Communications (PerCom)*, pp. 31–40, 2017. doi: 10.1109/PERCOM.2017.7917848.
 709
 710
 711
 712
 713
 714
- 715 Szegedy, C., Zaremba, W., Sutskever, I., Bruna, J., Erhan, D., Goodfellow, I. J., and Fergus, R. Intriguing properties of neural networks. In *2nd International Conference on Learning Representations, ICLR 2014, Banff, AB, Canada, April 14-16, 2014, Conference Track Proceedings*, 2014.
- 716 Tramer, F., Carlini, N., Brendel, W., and Madry, A. On adaptive attacks to adversarial example defenses, 2020.
 717
 718
 719 Uesato, J., O'Donoghue, B., Kohli, P., and van den Oord, A. Adversarial risk and the dangers of evaluating against weak attacks. In *Proceedings of the 35th International Conference on Machine Learning, ICML 2018, Stockholm, Sweden, July 10-15, 2018*, pp. 5032–5041, 2018.
 720
 721
 722 Vinitsky, E., Du, Y., Parvate, K., Jang, K., Abbeel, P., and Bayen, A. M. Robust reinforcement learning using adversarial populations. *CoRR*, abs/2008.01825, 2020. URL <https://arxiv.org/abs/2008.01825>.
 723
 724 Warden, P. Speech Commands: A Dataset for Limited-Vocabulary Speech Recognition. *ArXiv e-prints*, April 2018. URL <https://arxiv.org/abs/1804.03209>.
 725
 726
 727 Wong, E. and Kolter, J. Z. Provably robust defenses against adversarial examples via the convex outer adversarial polytope. In *Proceedings of the 35th International Conference on Machine Learning, ICML 2018, Stockholm, Sweden, July 10-15, 2018*, pp. 5283–5292, 2018.
 728
 729
 730 Wu, F., Li, L., Huang, Z., Vorobeychik, Y., Zhao, D., and Li, B. CROP: certifying robust policies for reinforcement learning through functional smoothing. *CoRR*, abs/2106.09292, 2021. URL <https://arxiv.org/abs/2106.09292>.
 731
 732
 733 Xu, H., Gao, Y., Yu, F., and Darrell, T. End-to-end learning of driving models from large-scale video datasets. In *2017 IEEE Conference on Computer Vision and Pattern Recognition, CVPR 2017, Honolulu, HI, USA, July 21-26, 2017*, pp. 3530–3538. IEEE Computer Society, 2017. doi: 10.1109/CVPR.2017.376. URL <https://doi.org/10.1109/CVPR.2017.376>.
 734
 735
 736 Yang, J. B., Nguyen, M. N., San, P. P., Li, X. L., and Krishnaswamy, S. Deep convolutional neural networks on multichannel time series for human activity recognition. In *Proceedings of the 24th International Conference on Artificial Intelligence, IJCAI'15*, pp. 3995–4001. AAAI Press, 2015. ISBN 9781577357384.
 737
 738
 739
 740
 741
 742
 743
 744
 745
 746
 747
 748
 749
 750
 751
 752
 753
 754
 755
 756
 757
 758
 759
 760
 761
 762
 763
 764
 765
 766
 767
 768
 769
 770
 771
 772
 773
 774
 775
 776
 777
 778
 779
 780
 781
 782
 783
 784
 785
 786
 787
 788
 789
 790
 791
 792
 793
 794
 795
 796
 797
 798
 799
 800
 801
 802
 803
 804
 805
 806
 807
 808
 809
 810
 811
 812
 813
 814
 815
 816
 817
 818
 819
 820
 821
 822
 823
 824
 825
 826
 827
 828
 829
 830
 831
 832
 833
 834
 835
 836
 837
 838
 839
 840
 841
 842
 843
 844
 845
 846
 847
 848
 849
 850
 851
 852
 853
 854
 855
 856
 857
 858
 859
 860
 861
 862
 863
 864
 865
 866
 867
 868
 869
 870
 871
 872
 873
 874
 875
 876
 877
 878
 879
 880
 881
 882
 883
 884
 885
 886
 887
 888
 889
 890
 891
 892
 893
 894
 895
 896
 897
 898
 899
 900
 901
 902
 903
 904
 905
 906
 907
 908
 909
 910
 911
 912
 913
 914
 915
 916
 917
 918
 919
 920
 921
 922
 923
 924
 925
 926
 927
 928
 929
 930
 931
 932
 933
 934
 935
 936
 937
 938
 939
 940
 941
 942
 943
 944
 945
 946
 947
 948
 949
 950
 951
 952
 953
 954
 955
 956
 957
 958
 959
 960
 961
 962
 963
 964
 965
 966
 967
 968
 969
 970
 971
 972
 973
 974
 975
 976
 977
 978
 979
 980
 981
 982
 983
 984
 985
 986
 987
 988
 989
 990
 991
 992
 993
 994
 995
 996
 997
 998
 999
 1000
 1001
 1002
 1003
 1004
 1005
 1006
 1007
 1008
 1009
 1010
 1011
 1012
 1013
 1014
 1015
 1016
 1017
 1018
 1019
 1020
 1021
 1022
 1023
 1024
 1025
 1026
 1027
 1028
 1029
 1030
 1031
 1032
 1033
 1034
 1035
 1036
 1037
 1038
 1039
 1040
 1041
 1042
 1043
 1044
 1045
 1046
 1047
 1048
 1049
 1050
 1051
 1052
 1053
 1054
 1055
 1056
 1057
 1058
 1059
 1060
 1061
 1062
 1063
 1064
 1065
 1066
 1067
 1068
 1069
 1070
 1071
 1072
 1073
 1074
 1075
 1076
 1077
 1078
 1079
 1080
 1081
 1082
 1083
 1084
 1085
 1086
 1087
 1088
 1089
 1090
 1091
 1092
 1093
 1094
 1095
 1096
 1097
 1098
 1099
 1100
 1101
 1102
 1103
 1104
 1105
 1106
 1107
 1108
 1109
 1110
 1111
 1112
 1113
 1114
 1115
 1116
 1117
 1118
 1119
 1120
 1121
 1122
 1123
 1124
 1125
 1126
 1127
 1128
 1129
 1130
 1131
 1132
 1133
 1134
 1135
 1136
 1137
 1138
 1139
 1140
 1141
 1142
 1143
 1144
 1145
 1146
 1147
 1148
 1149
 1150
 1151
 1152
 1153
 1154
 1155
 1156
 1157
 1158
 1159
 1160
 1161
 1162
 1163
 1164
 1165
 1166
 1167
 1168
 1169
 1170
 1171
 1172
 1173
 1174
 1175
 1176
 1177
 1178
 1179
 1180
 1181
 1182
 1183
 1184
 1185
 1186
 1187
 1188
 1189
 1190
 1191
 1192
 1193
 1194
 1195
 1196
 1197
 1198
 1199
 1200
 1201
 1202
 1203
 1204
 1205
 1206
 1207
 1208
 1209
 1210
 1211
 1212
 1213
 1214
 1215
 1216
 1217
 1218
 1219
 1220
 1221
 1222
 1223
 1224
 1225
 1226
 1227
 1228
 1229
 1230
 1231
 1232
 1233
 1234
 1235
 1236
 1237
 1238
 1239
 1240
 1241
 1242
 1243
 1244
 1245
 1246
 1247
 1248
 1249
 1250
 1251
 1252
 1253
 1254
 1255
 1256
 1257
 1258
 1259
 1260
 1261
 1262
 1263
 1264
 1265
 1266
 1267
 1268
 1269
 1270
 1271
 1272
 1273
 1274
 1275
 1276
 1277
 1278
 1279
 1280
 1281
 1282
 1283
 1284
 1285
 1286
 1287
 1288
 1289
 1290
 1291
 1292
 1293
 1294
 1295
 1296
 1297
 1298
 1299
 1300
 1301
 1302
 1303
 1304
 1305
 1306
 1307
 1308
 1309
 1310
 1311
 1312
 1313
 1314
 1315
 1316
 1317
 1318
 1319
 1320
 1321
 1322
 1323
 1324
 1325
 1326
 1327
 1328
 1329
 1330
 1331
 1332
 1333
 1334
 1335
 1336
 1337
 1338
 1339
 1340
 1341
 1342
 1343
 1344
 1345
 1346
 1347
 1348
 1349
 1350
 1351
 1352
 1353
 1354
 1355
 1356
 1357
 1358
 1359
 1360
 1361
 1362
 1363
 1364
 1365
 1366
 1367
 1368
 1369
 1370
 1371
 1372
 1373
 1374
 1375
 1376
 1377
 1378
 1379
 1380
 1381
 1382
 1383
 1384
 1385
 1386
 1387
 1388
 1389
 1390
 1391
 1392
 1393
 1394
 1395
 1396
 1397
 1398
 1399
 1400
 1401
 1402
 1403
 1404
 1405
 1406
 1407
 1408
 1409
 1410
 1411
 1412
 1413
 1414
 1415
 1416
 1417
 1418
 1419
 1420
 1421
 1422
 1423
 1424
 1425
 1426
 1427
 1428
 1429
 1430
 1431
 1432
 1433
 1434
 1435
 1436
 1437
 1438
 1439
 1440
 1441
 1442
 1443
 1444
 1445
 1446
 1447
 1448
 1449
 1450
 1451
 1452
 1453
 1454
 1455
 1456
 1457
 1458
 1459
 1460
 1461
 1462
 1463
 1464
 1465
 1466
 1467
 1468
 1469
 1470
 1471
 1472
 1473
 1474
 1475
 1476
 1477
 1478
 1479
 1480
 1481
 1482
 1483
 1484
 1485
 1486
 1487
 1488
 1489
 1490
 1491
 1492
 1493
 1494
 1495
 1496
 1497
 1498
 1499
 1500
 1501
 1502
 1503
 1504
 1505
 1506
 1507
 1508
 1509
 1510
 1511
 1512
 1513
 1514
 1515
 1516
 1517
 1518
 1519
 1520
 1521
 1522
 1523
 1524
 1525
 1526
 1527
 1528
 1529
 1530
 1531
 1532
 1533
 1534
 1535
 1536
 1537
 1538
 1539
 1540
 1541
 1542
 1543
 1544
 1545
 1546
 1547
 1548
 1549
 1550
 1551
 1552
 1553
 1554
 1555
 1556
 1557
 1558
 1559
 1560
 1561
 1562
 1563
 1564
 1565
 1566
 1567
 1568
 1569
 1570
 1571
 1572
 1573
 1574
 1575
 1576
 1577
 1578
 1579
 1580
 1581
 1582
 1583
 1584
 1585
 1586
 1587
 1588
 1589
 1590
 1591
 1592
 1593
 1594
 1595
 1596
 1597
 1598
 1599
 1600
 1601
 1602
 1603
 1604
 1605
 1606
 1607
 1608
 1609
 1610
 1611
 1612
 1613
 1614
 1615
 1616
 1617
 1618
 1619
 1620
 1621
 1622
 1623
 1624
 1625
 1626
 1627
 1628
 1629
 1630
 1631
 1632
 1633
 1634
 1635
 1636
 1637
 1638
 1639
 1640
 1641
 1642
 1643
 1644
 1645
 1646
 1647
 1648
 1649
 1650
 1651
 1652
 1653
 1654
 1655
 1656
 1657
 1658
 1659
 1660
 1661
 1662
 1663
 1664
 1665
 1666
 1667
 1668
 1669
 1670
 1671
 1672
 1673
 1674
 1675
 1676
 1677
 1678
 1679
 1680
 1681
 1682
 1683
 1684
 1685
 1686
 1687
 1688
 1689
 1690
 1691
 1692
 1693
 1694
 1695
 1696
 1697
 1698
 1699
 1700
 1701
 1702
 1703
 1704
 1705
 1706
 1707
 1708
 1709
 1710
 1711
 1712
 1713
 1714
 1715
 1716
 1717
 1718
 1719
 1720
 1721
 1722
 1723
 1724
 1725
 1726
 1727
 1728
 1729
 1730
 1731
 1732
 1733
 1734
 1735
 1736
 1737
 1738
 1739
 1740
 1741
 1742
 1743
 1744
 1745
 1746
 1747
 1748
 1749
 1750
 1751
 1752
 1753
 1754
 1755
 1756
 1757
 1758
 1759
 1760
 1761
 1762
 1763
 1764
 1765
 1766
 1767
 1768
 1769
 1770
 1771
 1772
 1773
 1774
 1775
 1776
 1777
 1778
 1779
 1780
 1781
 1782
 1783
 1784
 1785
 1786
 1787
 1788
 1789
 1790
 1791
 1792
 1793
 1794
 1795
 1796
 1797
 1798
 1799
 1800
 1801
 1802
 1803
 1804
 1805
 1806
 1807
 1808
 1809
 1810
 1811
 1812
 1813
 1814
 1815
 1816
 1817
 1818
 1819
 1820
 1821
 1822
 1823
 1824
 1825
 1826
 1827
 1828
 1829
 1830
 1831
 1832
 1833
 1834
 1835
 1836
 1837
 1838
 1839
 1840
 1841
 1842
 1843
 1844
 1845
 1846
 1847
 1848
 1849
 1850
 1851
 1852
 1853
 1854
 1855
 1856
 1857
 1858
 1859
 1860
 1861
 1862
 1863
 1864
 1865
 1866
 1867
 1868
 1869
 1870
 1871
 1872
 1873
 1874
 1875
 1876
 1877
 1878
 1879
 1880
 1881
 1882
 1883
 1884
 1885
 1886
 1887
 1888<br

715 learned optimal adversary. In *International Conference on Learning Representations*, 2021. URL <https://openreview.net/forum?id=sCZbhBvqQaU>.

716
717
718
719 Zhang, L., Aggarwal, C., and Qi, G.-J. Stock price
720 prediction via discovering multi-frequency trading pat-
721 terns. In *Proceedings of the 23rd ACM SIGKDD Inter-
722 national Conference on Knowledge Discovery and
723 Data Mining*, KDD '17, pp. 2141–2149, New York,
724 NY, USA, 2017. Association for Computing Machin-
725 ery. ISBN 9781450348874. doi: 10.1145/3097983.
726 3098117. URL <https://doi.org/10.1145/3097983.3098117>.

727

728

729

730

731

732

733

734

735

736

737

738

739

740

741

742

743

744

745

746

747

748

749

750

751

752

753

754

755

756

757

758

759

760

761

762

763

764

765

766

767

768

769

A. Proof of Lemma 5.1

Statement. The change in each \tilde{f}_j under an adversary in \mathcal{A}_ϵ is bounded as

$$|\tilde{f}_j(W_j) - \tilde{f}_j(W'_j)| \leq \sum_{i=j-w+1}^j \psi(d(x_i, x_i^{j+1-i})).$$

Proof. The left-hand side of the above inequality can be re-written as:

$$\begin{aligned} |\tilde{f}_j(W_j) - \tilde{f}_j(W'_j)| &= |\tilde{f}_j(x_{j-w+1}, \dots, x_j) - \tilde{f}_j(x_{j-w+1}^w, \dots, x_j^1)| \\ &= |\tilde{f}_j(x_{j-w+1}, \dots, x_{j-1}, x_j) - \tilde{f}_j(x_{j-w+1}, \dots, x_{j-1}, x_j^1) \\ &\quad + \tilde{f}_j(x_{j-w+1}, \dots, x_{j-1}, x_j^1) - \tilde{f}_j(x_{j-w+1}^w, \dots, x_{j-1}^2, x_j^1)| \\ &= \left| \sum_{k=1}^w \tilde{f}_j(x_{j-w+1}, \dots, x_{j-k+1}, x_{j-k+2}^{k-1}, \dots, x_j^1) - \tilde{f}_j(x_{j-w+1}, \dots, x_{j-k+1}^k, x_{j-k+2}^{k-1}, \dots, x_j^1) \right| \\ &\leq \sum_{k=1}^w \left| \tilde{f}_j(x_{j-w+1}, \dots, x_{j-k+1}, x_{j-k+2}^{k-1}, \dots, x_j^1) - \tilde{f}_j(x_{j-w+1}, \dots, x_{j-k+1}^k, x_{j-k+2}^{k-1}, \dots, x_j^1) \right| \end{aligned}$$

The two terms in each summand differ only in the $(j-k+1)$ -th input. Thus, it can be written as the difference of the expected value of some $[0, 1]$ -function q under the distributions $\mathcal{S}(x_{j-k+1})$ and $\mathcal{S}(x_{j-k+1}^k)$, i.e., $|\mathbb{E}_{\tilde{x}_{j-k+1} \sim \mathcal{S}(x_{j-k+1})}[q(\tilde{x}_{j-k+1})] - \mathbb{E}_{\tilde{x}_{j-k+1}^k \sim \mathcal{S}(x_{j-k+1}^k)}[q(\tilde{x}_{j-k+1}^k)]|$ which can be upper bounded by the total variation between $\mathcal{S}(x_{j-k+1})$ and $\mathcal{S}(x_{j-k+1}^k)$. Therefore, from condition (4), we have:

$$\begin{aligned} &|\tilde{f}_j(x_{j-w+1}, \dots, x_{j-k+1}, x_{j-k+2}^{k-1}, \dots, x_j^1) - \tilde{f}_j(x_{j-w+1}, \dots, x_{j-k+1}^k, x_{j-k+2}^{k-1}, \dots, x_j^1)| \\ &\leq \text{TV}(\mathcal{S}(x_{j-k+1}), \mathcal{S}(x_{j-k+1}^k)) \leq \psi(d(x_{j-k+1}, x_{j-k+1}^k)). \end{aligned}$$

This proves the statement of the lemma. \square

B. Proof of Theorem 5.2

Statement. Let \tilde{Z}_ϵ to be the minimum \tilde{Z} for an adversary in \mathcal{A}_ϵ . Then,

$$|\tilde{Z} - \tilde{Z}_\epsilon| \leq w\psi(\epsilon).$$

Proof. Let \tilde{Z}' be the overall performance of \tilde{M} under an adversary. Then,

$$\begin{aligned} |\tilde{Z} - \tilde{Z}'| &= \left| \frac{\sum_{j=1}^t \tilde{f}_j(W_j)}{t} - \frac{\sum_{j=1}^t \tilde{f}_j(W'_j)}{t} \right| \\ &\leq \frac{\sum_{j=1}^t |\tilde{f}_j(W_j) - \tilde{f}_j(W'_j)|}{t} \\ &\leq \sum_{j=1}^t \sum_{k=1}^w \psi(d(x_{j-k+1}, x_{j-k+1}^k))/t && \text{(from lemma 5.1)} \\ &\leq \sum_{j=1}^t \sum_{k=1}^w \psi(d(x_j, x_j^k))/t \\ &= w \sum_{j=1}^t \sum_{k=1}^w \psi(d(x_j, x_j^k))/wt \\ &\leq w\psi \left(\sum_{j=1}^t \sum_{k=1}^w d(x_j, x_j^k)/wt \right) && (\psi \text{ is concave and Jensen's inequality}) \end{aligned}$$

825 Therefore, for the worst-case adversary in \mathcal{A}_ϵ , we have
 826
 827

$$|\tilde{Z} - \tilde{Z}_\epsilon| \leq w\psi(\epsilon)$$

828 from constraint (2) on the average distance between the original and perturbed inputs. \square
 829

830 C. Function ψ for Different Distributions

831 For an isometric Gaussian distribution,
 832

$$834 \text{TV}(\mathcal{N}(x_i, \sigma^2 I), \mathcal{N}(x'_i, \sigma^2 I)) = \text{erf}(\|x_i - x'_i\|_2 / 2\sqrt{2}\sigma). \\ 835$$

836 *Proof.* Due to the isometric symmetry of the Gaussian distribution and the ℓ_2 -norm, the total variation between the two
 837 distributions is the same as when they are separated by the same ℓ_2 -distance but only in the first coordinate. It is equivalent
 838 to shifting a univariate normal distribution by the same amount. Therefore, the total variation between the two distributions
 839 is equal to the difference in the probability of a normal random variable with variance σ^2 being less than $\|x_i - x'_i\|_2/2$ and
 840 $-\|x_i - x'_i\|_2/2$, i.e., $\Phi(\|x_i - x'_i\|_2/2\sigma) - \Phi(-\|x_i - x'_i\|_2/2\sigma)$ where Φ is the standard normal CDF.
 841

$$\begin{aligned} 842 \text{TV}(\mathcal{N}(x_i, \sigma^2 I), \mathcal{N}(x'_i, \sigma^2 I)) &= \Phi(\|x_i - x'_i\|_2/2\sigma) - \Phi(-\|x_i - x'_i\|_2/2\sigma) \\ 843 &= 2\Phi(\|x_i - x'_i\|_2/2\sigma) - 1 \\ 844 &= 2\left(\frac{1 + \text{erf}(\|x_i - x'_i\|_2/2\sqrt{2}\sigma)}{2}\right) - 1 \\ 845 &= \text{erf}(\|x_i - x'_i\|_2/2\sqrt{2}\sigma). \\ 846 \\ 847 \\ 848 \end{aligned}$$

\square

851 For a uniform smoothing distribution $\mathcal{U}(x_i, b)$ between $x_{ij} - b/2$ and $x_{ij} + b/2$ in each dimension j of x_i for some $b \geq 0$,
 852 $\text{TV}(\mathcal{U}(x_i, b), \mathcal{U}(x'_i, b)) \leq \|x_i - x'_i\|_1/b$. When $\|x_i - x'_i\|_1$ is constrained, the overlap between $\mathcal{U}(x_i, b)$ and $\mathcal{U}(x'_i, b)$ is
 853 minimized when the shift is only along one dimension.
 854

855 D. Comparison with Existing Certificates for Static Tasks

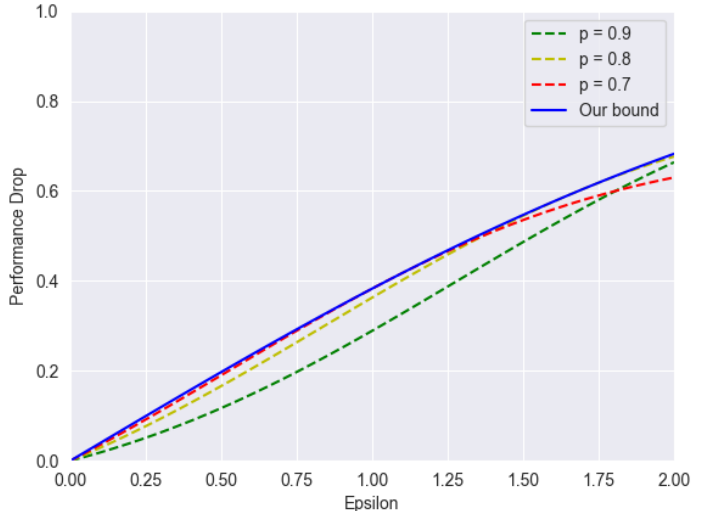
856 In this section, we compare our bound when applied to
 857 the static setting of classification, i.e., window size $w = 1$
 858 in bound (1), to that obtained by Cohen et al. (2019) for
 859 an ℓ_2 adversary and a Gaussian smoothing distribution.
 860 As discussed in Appendix C, the ψ function for this case
 861 takes the form of the Gauss error function erf. Thus our
 862 bound on the drop in the smoothed model's performance
 863 against an ℓ_2 adversary is given by:
 864

$$865 |\tilde{Z} - \tilde{Z}_\epsilon| \leq \text{erf}(\epsilon/2\sqrt{2}\sigma). \\ 866$$

867 Cohen et al. (2019)'s certificate bounds the worst-case
 868 adversarial performance as a function of the clean performance.
 869 If the probability of predicting the correct class
 870 is p on the original input, the probability of that in the
 871 presence of an adversary is bounded by $\Phi(\Phi^{-1}(p) - \epsilon/\sigma)$.
 872 Therefore, the performance drop Δp is bounded by:
 873

$$874 \Delta p \leq p - \Phi\left(\Phi^{-1}(p) - \frac{\epsilon}{\sigma}\right). \quad (5) \\ 875$$

876 Figure 6 compares the two bounds for different values of
 877 p . We keep $\sigma = 1$ as it only has a scaling effect along the
 878 879



875 Figure 6. Comparison between our bound and Cohen et al. (2019)'s
 876 certificate for an ℓ_2 adversary and a Gaussian smoothing distribution.
 877 The solid blue curve corresponds to our bound and the dashed curves
 878 represent bound (5) for different values of p . We keep $\sigma = 1$ as it
 879 only has a scaling effect along the x -axis.

880 x -axis. The bound from the ℓ_2 certificate by Cohen et al. (2019) is tighter than ours, mainly because it takes the clean
881 performance p of the smoothed model into account. However, the gap between the two bounds is small in the range where ϵ
882 goes from 0 to 2, by which point the certified performance drops by more than 60%. Thus for most meaningful robustness
883 guarantees, our certificates are almost at par with the best-known ℓ_2 certificates. The key advantage of our certificates over
884 those for the static setting is that they are applicable for an adaptive adversary that can allocate different attack budgets for
885 different input items in the stream.
886

887 E. Experimental details

888 We use a single NVIDIA RTX A4000 GPU with four AMD EPYC 7302P Processors. For our main experiments with UCI
889 HAR and Speech Commands datasets, we use window size $w = 2$ with inputs belonging to $\mathbb{R}^{250 \times 6}$ and \mathbb{R}^{4000} . The UCI
890 HAR dataset consists of long streaming inputs with sample-level annotations. For a window W_j , the label is the majority
891 class that is present in that window. The signals in the HAR dataset are standardized to have mean 0 and variance 1. For
892 the speech keyword detection task, we use a subset of the Speech commands dataset that consists of long noise clips and
893 one-second-long speech keyword clips. The labels for each audio clip are available. We utilize all the long noise clips
894 and clips belonging to the classes belonging speech utterances of numbers from zero to nine to make longer clips for our
895 streaming case. We add noise clips to the keyword audios to make them more similar to real-world scenarios. Each clip
896 is stitched together (Li et al., 2018) with arbitrarily long noise between each keyword clip. To make transitions between
897 the audio smooth, we use exponential decays to overlap keyword audio clips for stitching, with noise in the background.
898 Hence, for the speech keyword detection, we have 11 classes for labels – zero to nine and a noise class. A window is labeled
899 to be the majority class in that window.
900

901 For training, we use M5 networks with 32 channels for HAR. We train for 30 epochs with a bath-size of 256 using SGD
902 with an initial learning rate of 0.1, momentum of 0.9, and weight decay of 0.0001. We use a cosine annealing learning rate
903 scheduler. For training the robust models, we use different smoothing noises with standard deviations 4, 6, 8, and 10. For
904 training on the keyword detection data, we use M5 networks with 128 channels for HAR. We train for 30 epochs with a
905 bath-size of 128 using SGD with an initial learning rate of 0.1, momentum of 0.9, and weight decay of 0.0001. We use a
906 cosine annealing learning rate scheduler. For training the robust models, we use different smoothing noises with standard
907 deviations 0.1, 0.2, 0.4, 0.6, and 0.8. For attacking the trained models, we use PGD ℓ_2 attacks for both the datasets. PGD is
908 run for 100 steps with a step size of $2\epsilon'/100$ where ϵ' is the ℓ_2 attack budget.
909

910 F. Attacking the Smooth Models

911 In this section, we empirically demonstrate that the performance of our smooth models in the presence of an adversary is
912 lower bound by the certificates we obtain. For these experiments, we consider an adversary that can only attack an input
913 once, as in Section 6.1. We show our results on the Human Activity Recognition dataset in Figure 7 and the keyword
914 detection task in Figure 8 for a window size of $w = 2$. As seen in the plots, the empirical performance of the smooth models
915 after the online adversarial attack is always better than our theoretical certificates. Hence, this experiment validates our
916 certificates.
917

918
919
920
921
922
923
924
925
926
927
928
929
930
931
932
933
934

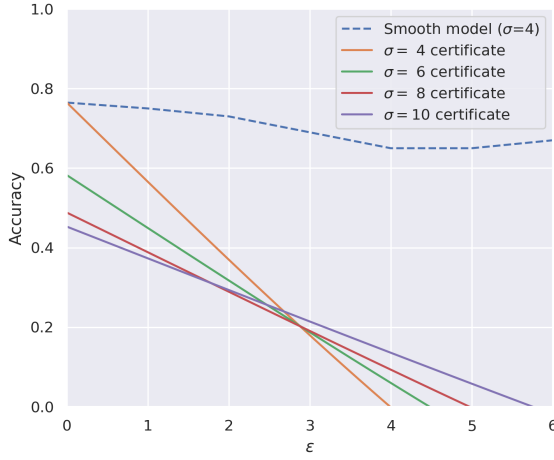
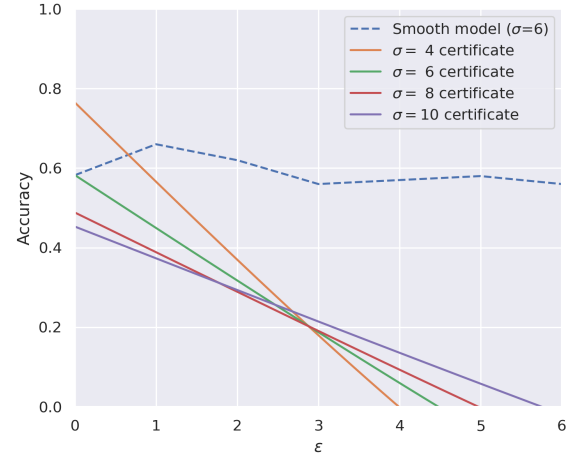
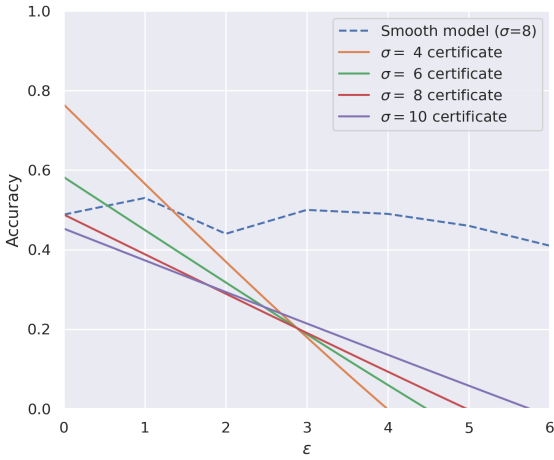
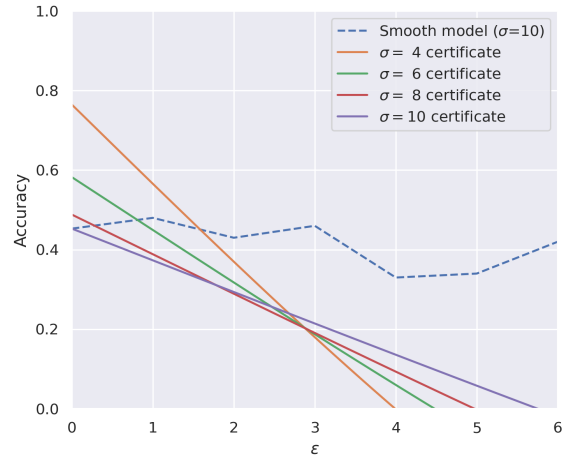
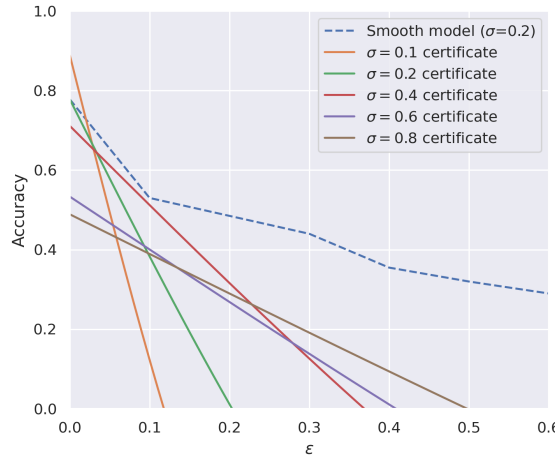
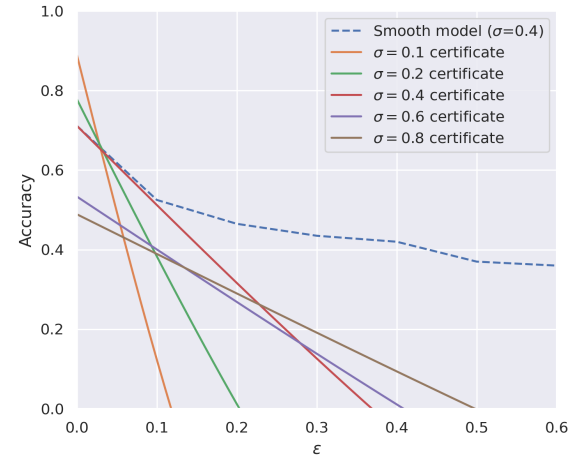

 (a) Attacking model with smoothing noise $\sigma = 4$

 (b) Attacking model with smoothing noise $\sigma = 6$

 (c) Attacking model with smoothing noise $\sigma = 8$

 (d) Attacking model with smoothing noise $\sigma = 10$

Figure 7. Certificates against online adversarial attacks for varying smoothing noises for the speech keyword detection task. We attack smooth models trained with different smoothing noises in these plots. Here we can perturb each input only once. The average size of perturbation is computed as per equation 2.

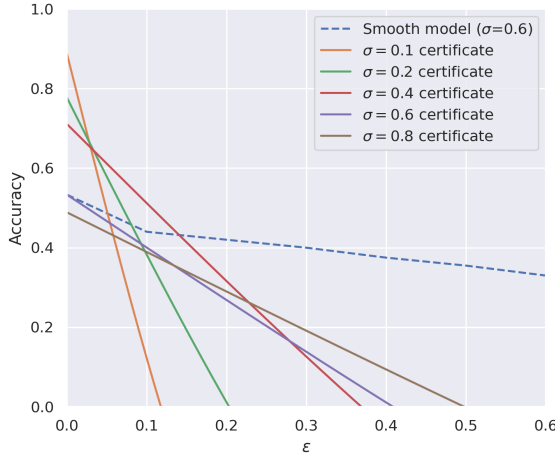
990
 991
 992
 993
 994
 995
 996
 997
 998
 999
 1000
 1001
 1002
 1003
 1004
 1005
 1006
 1007
 1008
 1009
 1010
 1011
 1012
 1013
 1014
 1015
 1016
 1017
 1018
 1019
 1020
 1021
 1022
 1023
 1024
 1025
 1026
 1027
 1028
 1029
 1030
 1031
 1032
 1033
 1034
 1035
 1036
 1037
 1038
 1039
 1040
 1041
 1042
 1043
 1044



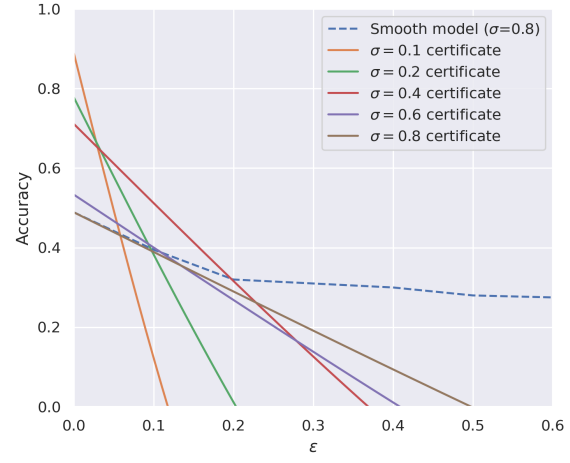
(a) Attacking model with smoothing noise $\sigma = 0.2$



(b) Attacking model with smoothing noise $\sigma = 0.4$



(c) Attacking model with smoothing noise $\sigma = 0.6$



(d) Attacking model with smoothing noise $\sigma = 0.8$

Figure 8. Certificates against online adversarial attacks for varying smoothing noises for the speech keyword detection task. We attack smooth models trained with different smoothing noises in these plots. Here we can perturb each input only once. The average size of perturbation is computed as per equation 2.